OPEN ACCESS

KING'S College LONDON

King's Research Portal

Document Version
Peer reviewed version

Link to publication record in King's Research Portal

Citation for published version (APA):
Bustin, A., Milotta, G., Ismail, T. F., Neji, R., Botnar, R. M., & Prieto Vasquez, C. (Accepted/In press). Accelerated free-breathing whole-heart 3D T2 mapping with high isotropic resolution. *Magnetic Resonance in Medicine*.

Citing this paper
Please note that where the full-text provided on King's Research Portal is the Author Accepted Manuscript or Post-Print version this may differ from the final Published version. If citing, it is advised that you check and use the publisher's definitive version for pagination, volume/issue, and date of publication details. And where the final published version is provided on the Research Portal, if citing you are again advised to check the publisher's website for any subsequent corrections.

General rights
Copyright and moral rights for the publications made accessible in the Research Portal are retained by the authors and/or other copyright owners and it is a condition of accessing publications that users recognize and abide by the legal requirements associated with these rights.

•Users may download and print one copy of any publication from the Research Portal for the purpose of private study or research.
•You may not further distribute the material or use it for any profit-making activity or commercial gain
•You may freely distribute the URL identifying the publication in the Research Portal

Take down policy
If you believe that this document breaches copyright please contact librarypure@kcl.ac.uk providing details, and we will remove access to the work immediately and investigate your claim.

Download date: 06. May. 2023

Accelerated free-breathing whole-heart 3D T2 mapping with high isotropic resolution

Journal:	*Magnetic Resonance in Medicine*
Manuscript ID	MRM-19-19913.R2
Wiley - Manuscript type:	Full Paper
Date Submitted by the Author:	n/a
Complete List of Authors:	Bustin, Aurélien; King's College London, Department of Biomedical Engineering, School of Biomedical Engineering and Imaging Sciences, Milotta, Giorgia; King's College London, Department of Biomedical Engineering, School of Biomedical Engineering and Imaging Sciences Ismail, Tevfik; King's College London, Department of Biomedical Engineering, School of Biomedical Engineering and Imaging Sciences Neji, Radhouene; King's College London, Department of Biomedical Engineering, School of Biomedical Engineering and Imaging Sciences; Siemens Healthcare Limited, MR Research Collaborations Botnar, Rene; King's College London, Department of Biomedical Engineering, School of Biomedical Engineering and Imaging Sciences; Pontificia Universidad Católica de Chile, Escuela de Ingeniería Prieto, Claudia; King's College London, Department of Biomedical Engineering, School of Biomedical Engineering and Imaging Sciences; Pontificia Universidad Católica de Chile, Escuela de Ingeniería
Research Type:	T2 < Relaxation techniques < Technique Development < Technical Research, Reconstruction < Technique Development < Technical Research
Research Focus:	Heart < Cardiovascular

SCHOLARONE™
Manuscripts

Accelerated Free-Breathing Whole-Heart 3D T2 Mapping with High Isotropic Resolution

Aurélien Bustin[1], Giorgia Milotta[1], Tevfik F. Ismail[1], Radhouene Neji[1,2], René M. Botnar[1,3], Claudia Prieto[1,3]

[1]Department of Biomedical Engineering, School of Biomedical Engineering and Imaging Sciences, King's College London, London, United Kingdom
[2]MR Research Collaborations, Siemens Healthcare Limited, Frimley, United Kingdom
[3]Escuela de Ingeniería, Pontificia Universidad Católica de Chile, Santiago, Chile

For Peer Review

Short Title: Free-Breathing Whole-Heart 3D T_2 Mapping
Submitted as Full Paper to Journal of Magnetic Resonance in Medicine
Main document word count: 5140

Corresponding author:

Name Aurélien Bustin, PhD
School of Biomedical Engineering and Imaging Sciences
King's Health Partners, King's College London
Address 3rd Floor, Lambeth Wing, St Thomas' Hospital
London SE1 7EH
United Kingdom
E-mail aurelien.bustin@kcl.ac.uk

ABSTRACT

Purpose: To enable free-breathing whole-heart 3D T2 mapping with high isotropic resolution in a clinically feasible and predictable scan time. This 3D Motion-corrected Undersampled Signal maTched (MUST)-T2 map is achieved by combining an undersampled motion-compensated T2-prepared Cartesian acquisition with a high-order patch-based reconstruction.

Methods: 3D MUST-T2 mapping acquisition consists of an ECG-triggered, T2-prepared, balanced steady-state free precession sequence with non-selective saturation pulses. Three undersampled T2-weighted volumes are acquired using a 3D Cartesian variable-density sampling with increasing T2 preparation times. A 2D image-based navigator is used to correct for respiratory motion of the heart and allow 100% scan efficiency. Multi-contrast HD-PROST reconstruction is used in concert with dictionary matching to generate 3D T2 maps. The proposed framework was evaluated in simulations, phantom experiments, and in vivo (10 healthy subjects, 2 patients) with 1.5mm^3 isotropic resolution. 3D MUST-T2 was compared against standard multi-echo spin-echo sequence (phantom) and conventional breath-held single-shot 2D SSFP T2 mapping (in-vivo).

Results: 3D MUST-T2 showed high accuracy in phantom experiments (R^2>0.99). The precision of T2 values was similar for 3D MUST-T2 and 2D bSSFP T2 mapping in-vivo (5±1ms vs. 4±2ms, *P*=0.52). Slightly longer T2 values were observed with 3D MUST-T2 in comparison to 2D bSSFP T2 mapping (50.7±2ms vs. 48.2±1ms, P<0.05). Preliminary results in patients demonstrated T2 values in agreement with literature values.

Conclusion: The proposed approach enables free-breathing whole-heart 3D T2 mapping with high isotropic resolution in ~8 min, achieving accurate and precise T2 quantification of myocardial tissue in a clinically feasible scan time.

Keywords: myocardial T2 mapping, T2 quantification, fast imaging, motion correction, isotropic resolution

For Peer Review

INTRODUCTION

Quantitative myocardial T2 mapping has emerged as a promising tool for edema characterization and detection of subtle myocardial inflammation in patients with acute myocardial infarction, myocarditis, dilated cardiomyopathy, sarcoidosis, and autoimmune cardiomyopathies (1–4).

Myocardial T2 mapping is usually performed by acquiring several ECG-triggered T2-weighted (T2w) images, with different amounts of T2 decay through T2-preparation pulses. A map of T2 relaxation times is then generated by fitting the series of weighted images to an exponential decay model on a pixel-by-pixel basis. Current clinical protocols usually perform myocardial T2 mapping with a two-dimensional (2D) single-shot steady-state free-precession sequence (T2p-SSFP), acquiring three T2-prepared images in a single-breathold every two to three heartbeats to allow for full T1 recovery (3). Multiple short-axis slices are usually acquired at the basal, mid-ventricular and apical level.

However, the use of 2D acquisitions with fairly thick slices and the associated partial volume effects undermine the full potential of myocardial T2 mapping, particularly in hypertrophic cardiomyopathies where the pathological tissues are often complex three-dimensional structures with differing T2 values (5–7). Furthermore, 2D sequences, typically acquired during breath holding, regularly suffer from respiratory and cardiac motion between the T2w images, mainly due to imperfect breath-holding or variable heart rate (8). Although robust non-rigid motion-correction techniques have been proposed to correct for residual motion and improve map quality, such techniques are relatively complex, computationally expensive and only correct for in-plane motion (9–11).

A free-breathing 3D T2 mapping approach with high isotropic spatial resolution may have the potential to increase diagnostic accuracy in patients with acute myocardial injury (e.g., NSTEMI patients (12,13)), and improve the detection of cardiac involvement in patients with systemic sarcoidosis (14).

For Peer Review

Three-dimensional (3D) myocardial T2 mapping techniques have been proposed to address the limitations of 2D imaging by allowing for large coverage of the heart with inherently higher signal-to-noise ratio (SNR). Non-cartesian self-navigated myocardial T2 mapping has been proposed to perform free-breathing 3D myocardial T2 mapping at 3T in ~18 min acquisition time (5,15). Such long scan times, unfortunately, may impede the clinical integration of this technique. A self-navigated hybrid radial-cartesian trajectory was also proposed to perform free-breathing 3D myocardial T2 mapping in less than 5 min, however with low spatial resolution (16). The use of saturation pulses at every heartbeat was proposed to accelerate Cartesian 3D T2 mapping (17). Long resting periods (in the order of 2-3 heartbeats (3,5) are usually needed in T2 mapping to ensure full recovery of the longitudinal magnetization between acquisitions to minimize T1 effects and satisfy the assumption that the equilibrium state magnetization is not affected by heart rate variations throughout the scan. Non-selective 90° saturation pulses reset magnetization history by tipping the longitudinal magnetization of the imaged volume into the transverse plane, thus removing heart rate dependency during the acquisition and allowing for imaging every heartbeat. This approach also eliminates artifacts caused by heart rate variations, at the cost of a reduced SNR and lower precision of T2 values. However, this technique uses prospective diaphragmatic navigator-gated (dNAV) acquisitions and thus leads to prolonged and often unpredictable scan times (~9 min nominal scan time with 30% to 60% respiratory gating efficiency) since only a small fraction of the acquired data is accepted for reconstruction (referred to as low scan efficiency).

Notwithstanding the continued advancements, myocardial 3D T2 mapping still faces substantial technical challenges which in turn may limit its applicability in clinical practice. In this study, we sought to achieve high isotropic spatial resolution 3D Cartesian whole-heart myocardial T2 mapping in a short and predictable scan time of ~8 min by combining a highly accelerated saturation-based free-breathing myocardial T2 mapping sequence with 2D image-based navigator (iNAV) based respiratory motion correction. A recently proposed high-dimensionality undersampled patch-based reconstruction (HD-PROST) (18) is employed in concert with dictionary matching, based on the Extended Phase Graph

(EPG) formalism (19), to allow for accurate and precise myocardial T2 maps. The proposed framework was validated in simulations, phantom and healthy subject experiments, while its initial clinical feasibility was shown for two patients with suspected cardiovascular disease.

METHODS

Acquisitions were performed on a 1.5T MR scanner (Magnetom Aera, Siemens Healthcare, Erlangen, Germany) with a dedicated 18-channel body coil and a 32-channel spine coil. Written informed consent was obtained from all healthy subjects and patients before undergoing MRI scans and the study was approved by the National Research Ethics Service. Numerical simulations, reconstructions and analysis were performed on a workstation with a 16-core Dual Intel Xeon Processor (2.3 GHz, 256GB RAM).

Accelerated Whole-heart 3D T2 Mapping Sequence

The proposed myocardial 3D Motion corrected Undersampled Signal maTched (MUST)-T2 mapping sequence is shown in Figure 1. A saturation pulse is performed right after the R-wave with a constant T_{SAT} time from the data acquisition. T_{SAT} is set to the maximal available time allowed by the sequence to guarantee enough magnetization recovery before the next acquisition. This approach allows efficient imaging at every heartbeat, avoiding the use of multiple recovery periods (17). Subsequently, an adiabatic T2 prepared pulse with variable echo time (TE_{T2prep}) is performed, followed by a balanced steady-state free-precession (bSSFP) read-out. An adiabatic T2-prep module (Silver-Hoult type) is employed due its good insensitivity to B1 and B0 inhomogeneities (20). Three T2w volumes are acquired sequentially with different T2-weightings (TE_{T2prep} = [0, 28, 55] ms).

A 3D Cartesian variable-density trajectory with spiral profile order (VD-CASPR) (21,22) is employed to allow for fast acquisition of the three T2-prepared volumes. This trajectory samples the k_y-k_z phase-encoding plane following approximate spiral interleaves on the Cartesian grid with variable density along each spiral arm and with two successive spiral interleaves being rotated by the golden angle. A golden angle rotation (21,23) between

For Peer Review

different contrast acquisitions was incorporated to introduce incoherently distributed aliasing along the contrast dimension and noise-like artifacts in the spatial dimension (Supporting Information Figure S1).

A 2D low-resolution iNAV (24) precedes the 3D acquisition at every heartbeat to enable 2D translational respiratory motion estimation/compensation (superior-inferior and right-left directions). This technique, already validated for coronary MR angiography (24) and multi-contrast cardiac MRI (25), enables 100% scan efficiency with predictable scan time, resulting in ~2-3 times acceleration compared to dNAV-based acquisitions. 2D iNAVs are obtained by spatially encoding the startup echoes of the bSSFP T2 mapping sequence. 2D translational motion is estimated using a template-matching algorithm with normalized cross-correlation as similarity measure, with the template manually selected around the heart during acquisition planning. Motion compensation of the three volumes is performed by modulating the k-space data with a linear phase shift to a reference respiratory position selected at end-expiration (24).

Multi-Contrast HD-PROST Reconstruction

Multi-contrast HD-PROST (18,22) is employed to reconstruct the three undersampled T2w volumes. HD-PROST exploits local (i.e., within a patch), non-local (i.e., between similar patches within a neighborhood) and contrast (i.e., between T2w images) redundancies of the 3D volumes in an efficient low-rank formulation. The reconstruction is formulated as an iterative two-step process: 1) an L2-norm regularized parallel-imaging reconstruction using the denoised multi-contrast data from step 2 as a prior (optimization 1), and 2) an efficient high-order low-rank patch-based denoising (optimization 2, Supporting Information Figure S2). The first step is optimized by gradient descent, whereas the second step is optimized through high-order low-rank tensor decomposition. The performance of HD-PROST reconstruction relies mainly on two parameters that need to be carefully tuned in order to get the best reconstruction quality: i) the patch size ($N = 5 \times 5 \times 5$ pixels in this study), reflecting the degree of structural information within each patch; and ii) the high-

For Peer Review

order singular value truncation parameter ($\lambda_p = 0.1$ in this study) which controls the amount of regularization.

HD-PROST reconstruction was implemented and performed offline using the algorithm described in (18). Reconstruction parameters were empirically optimized (as previously reported) and are illustrated in Supporting Information Figure S2. We refer the reader to (18,26) for a detailed description of HD-PROST and the associated reconstruction parameters.

Numerical Simulations

Usually in myocardial T2 mapping, the acquisition of each T2-weighted image is followed by a resting period of ~2-3 heartbeats to allow for full longitudinal magnetization relaxation. Numerical EPG simulations were first performed to investigate the impact of removing recovery heartbeats, and integrating saturation pulses, on the longitudinal magnetization of 3D MUST-T2 for tissues with different relaxation times T1. Simulations were performed for a T2 of 50 ms and varying T1 values (ranging from 700 ms to 1200 ms) with and without saturation pulses. Other relevant parameters used in the simulations were TE_{T2prep} = 55 ms, repetition time (TR) = 3.2 ms, trigger delay = 856 ms, data-acquisition window of 100 ms, and a simulated heart rate of 60 beats per minute (bpm).

Dictionary Generation and Matching

3D MUST-T2 dictionaries are simulated using the EPG formalism (19,27,28) for a range of T2 values. For both phantom and in vivo experiments, the dictionaries are calculated matching the subject-specific acquisition parameters with T2s in the range [minimum: step size: maximum] of [4:2:100, 105:5:200, 210:10:450] ms. Simulations show that the proposed method is not dependent on the used T1 value (in the range of interest) for dictionary generation (Supporting Information Figure S3, where the simulation results are shown for different T1 values ranging from 850 ms to 1200 ms with a step size of 50 ms), thus T1 is kept constant at 1100 ms for the phantom and in-vivo experiments. T2 maps are obtained by voxel-wise matching of the measured and normalized signal to the closest

For Peer Review

(minimum least square) EPG-based dictionary entry. The choice of dictionary-based matching versus conventional mono-exponential curve fitting is justified in Supporting Information Figure S4.

Phantom Experiments

The proposed ECG-triggered 3D MUST-T2 mapping sequence was evaluated in a standardized (T1MES) T1/T2 phantom containing nine agarose-based tubes with relevant cardiac T1 and T2 combinations (range, T1: 255 ms to 1489 ms, T2: 44 ms to 243 ms) (29). Scan parameters for 3D MUST-T2 included: TR = 3.13 ms, echo time (TE) = 1.37 ms, flip angle (FA) = 90°, field-of-view (FOV) = 187x187x156 mm^3, 1.5 mm^3 isotropic resolution, bandwidth (BW) = 908 Hz/pixel, data-acquisition window = 100 ms, TE_{T2prep} = [0, 28, 55] ms. Reference T2 relaxation times for each vial were obtained using a multi-echo spin-echo (SE) sequence with eight TEs ranging from 10 ms to 640 ms. In addition, conventional ECG-triggered 2D T2p-SSFP was performed for comparison purposes with the following imaging parameters: 1.9 x 1.9 mm^2 in-plane resolution, slice thickness = 8 mm, TR/TE = 3.11/1.38 ms, linear k-space reordering, BW = 1184 Hz/pixel, TE_{T2prep} = [0, 25, 55] ms, FA = 70°, 3 recovery beats, GRAPPA factor 2 with 36 k-space auto-calibration lines. The T2 relaxation times were obtained by mono-exponential curve fitting for both SE and T2p-SSFP sequences.

Impact of heart rate on T2 accuracy

The impact of heart rate differences on T2 accuracy was assessed by performing multiple 3D MUST-T2 phantom acquisitions with different simulated heart rates (ranging from 50 bpm to 100 bpm, step size 10 bpm). The trigger delay was set to 70% of the R-R interval and ranged from 420 ms to 840 ms, while the saturation time T_{SAT} was always set to the maximum allowed time (ranging from 370 ms to 790 ms). The acquisitions were performed fully sampled using the previously described VD-CASPR sampling.

Impact of acceleration on T2 accuracy

For Peer Review

To study the impact of accelerating 3D MUST-T2 on the accuracy of the T2 values, several phantom acquisitions were performed with different undersampling factors ranging from 1-fold to 5-fold (step size 1). Additional acquisition parameters included: simulated heart rate of 60 bpm, trigger delay of 680 ms, and saturation time T_{SAT} = 630 ms.

Data Analysis

Circular regions of interest were drawn on each vial for 3D MUST-T2, SE and 2D T2p-SSFP sequences. For each vial, the average T2 value was measured and agreement between SE, 2D T2p-SSFP T2 values and the proposed approach was assessed using linear regression.

In Vivo Experiments

Healthy Subjects

Ten healthy subjects (5 men and 5 women, mean age: 30-year-old, range: 26-36 years) with no history of cardiovascular disease underwent ECG-triggered free-breathing 3D whole-heart T2 mapping using the proposed 3D MUST-T2 acquisition approach. Relevant scan parameters included: FOV = 320 x 320 x 84-108 mm^3, slice-oversampling 22%, 1.5 mm^3 isotropic resolution, FA = 90°, TE_{T2prep} = [0, 28, 55] ms, subject-dependent mid-diastolic trigger delay (mean: 672 ms, range: 521-952 ms), acquisition window (mean: 97 ms, range: 80-108 ms), T_{SAT} (range: 470-900 ms), acceleration factor of 5x, 14 linear ramp-up pulses for iNAV, and Hanning-filtered sinc pulse with a duration of 1 ms and time-bandwidth product of 4.5. To ensure adequate fat suppression, a spectral pre-saturation with inversion recovery (SPIR) was applied before imaging. All 3D MUST-T2 mapping acquisitions were performed in the coronal plane.

Conventional 2D T2p-SSFP T2 mapping (3) was acquired for each subject for comparison purposes. Acquisition parameters were the same as for the phantom experiments. Three short-axis slices (basal, mid-cavity, apical) were acquired in three separate breath-holds of ~10 seconds each. A non-rigid motion correction was carried out inline to compensate for

For Peer Review

in-plane motion between the three 2D T2w images (11). Subsequently, T2 maps were obtained by mono-exponential curve fitting.

Patients

The feasibility and preliminary clinical performance of the proposed 3D MUST-T2 sequence was assessed in two patients (2 men, age: 42-year-old and 50-year-old) with suspected cardiovascular disease. The same acquisition and reconstruction parameters as in the healthy subject study were used. The patient-specific saturation times were T_{SAT} = 525 ms (patient #1, average heart rate: 75 bpm, acquisition window = 98 ms) and T_{SAT} = 595 ms (patient #2, average heart rate: 65 bpm, acquisition window = 100 ms). Conventional 2D T2p-SSFP T2 mapping was acquired for each patient with same parameters as in the healthy subject study.

Data Analysis

3D MUST-T2 maps were reformatted in the short-axis view to match the 2D T2p-SSFP slices. Regional differences in left ventricular T2 relaxation times were assessed according to the 16-segment model of the American Heart Association (AHA) (30). T2 measurements were reported as mean ± standard deviation and assessed using Student's t-test. Statistical differences in regional T2 values among reformatted basal, mid-ventricular and apical short-axis slices were analyzed using repeated-measures one-way analysis of variance (ANOVA) with Bonferroni post-hoc comparisons. All statistical analyses were performed using MATLAB (v7.1, The MathWorks, Natick, MA), and statistical significances were defined as a P value < 0.05.

RESULTS

Numerical Simulations

The impact of recovery times on the signal intensity (longitudinal magnetization) is depicted in Figure 2a-b for multiple T1 relaxation times (ranging from 700 ms to 1200 ms). While a clear dependency was observed when no saturation pulse is applied, necessitating

For Peer Review

~2-3 resting periods to recover 96% of the signal intensity (Figure 2a), applying a 'reset' saturation pulse (17) at every heartbeat avoids recovery periods, at the cost of a lower signal intensity (Figure 2b).

Phantom Experiments

Average T2 values obtained in the phantom experiments when increasing the simulated heart rate (from 50 bpm to 100 bpm) are depicted in Figure 2c. T2 relaxation times measured with the proposed 3D MUST-T2 sequence showed no to little sensitivity to change of heart rate for all vials in comparison to SE reference measurements.

Accuracy of the T2 values obtained with the proposed 3D MUST-T2 approach in phantom is shown in Figure 3 for different acceleration factors. Excellent linear correlation was found between 3D MUST-T2 and the ground-truth T2 values obtained with SE, with high coefficients of determination ($R^2 > 0.99$) for all acceleration factors (1x to 5x), suggesting high accuracy of the proposed 3D sequence even for high acceleration factors. Lower linear correlation ($R^2 = 0.95$) was observed for conventional 2D T2p-SSFP in comparison to reference SE measurements. Bias between SE and 2D T2p-SSFP with linear order acquisitions has been reported previously (3).

Bland-Altman analysis demonstrated good T2 agreement for all 31 slices of 3D MUST-T2 (Supporting Information Figure S5). The mean differences with 95% confidence interval (CI) between 3D MUST-T2 and SE were 0.6 ms (95% CI, -2.1 ms to 0.89 ms) for short T1 myocardium ([T2,T1] = [48,803] ms), 0.6 ms (95% CI, -3.7 to 2.5 ms to ms) for medium T1 myocardium ([T2,T1] = [48,1090] ms), and 1.4 ms (95% CI, -4.9 ms to -2.0 ms) for long T1 myocardium ([T2,T1] = [50,1333] ms).

In Vivo Experiments

All healthy subject and patient acquisitions/reconstructions were performed successfully, and analysis results are reported hereafter.

Healthy Subjects

For Peer Review

The average acquisition time of the proposed free-breathing 3D MUST-T2 sequence in healthy subjects was 6min43s ± 1min37s (range 4–10 minutes, heart rate range: 38–85 bpm) with 100% scan efficiency. Translational motion estimation and correction was performed in about 20s, while the average reconstruction time (including HD-PROST reconstruction and dictionary matching) was about 3 min. Representative T2 maps from three healthy subjects acquired with the proposed 3D MUST-T2 sequence and the conventional 2D T2p-SSFP sequence are shown in Figure 4. Both free-breathing 3D MUST-T2 and breath-held 2D T2p-SSFP show comparable visualization of the left ventricle and surrounding structures (e.g., papillary muscles). Reconstructed T2 maps from additional healthy subjects are shown in Supporting Information Figure S6 and Supporting Information Figure S7.

Bull's eye plots based on the AHA's 16-segment model of the left ventricle obtained with 3D MUST-T2 and 2D T2p-SSFP mappings are depicted in Figure 5a. A small, although significant, overestimation of regional T2 values, over the whole myocardium, was observed with 3D MUST-T2 in comparison to 2D T2p-SSFP mapping (50.7 ± 1.7 ms for 3D MUST-T2 versus 48.2 ± 1.3 ms for 2D T2p-SSFP, $P < 0.05$). We found no statistical differences in regional T2 values between segments with 3D MUST-T2 for all subjects ($P = 0.6$). A small overestimation of septal T2 values was observed with 3D MUST-T2 in comparison to 2D T2p-SSFP mapping with linear k-space reordering (mean difference: -4.2 ms, ±95% confidence interval: -10.4/2.0 ms, Figure 5b). Precision of T2 values was similar for both techniques (5 ± 1 ms for 3D MUST-T2 versus 4 ± 2 ms for 2D T2p-SSFP, $P = 0.520$, Figure 5c). The corresponding average coefficient of variation for the proposed 3D MUST-T2 approach was similar to that of the 2D conventional sequence (9.13% versus 9.09%, respectively, $P = 0.097$). There were no statistical differences in mean T2 values with 3D MUST-T2 among basal, mid-ventricular and apical slices for all subjects ($P = 0.655$).

The effect of heart rate differences across healthy subjects on T2 values is shown in Figure 2d. T2 measurements obtained from 3D MUST-T2 in vivo showed no significant correlation with heart rate ($T2 = 0.026 \times heart\ rate + 49$ ms, $P = 0.919$).

For Peer Review

Eight short-axis slices of the left ventricular myocardium for one representative healthy subject obtained with the proposed 3D MUST-T2 approach are shown in Figure 6. The reconstructed T2w images and the corresponding T2 maps are included. No noticeable residual undersampling artifacts were observed on the native T2w images, and corresponding T2 maps, for the entire left ventricle.

Since MUST-T2 acquisitions were performed with isotropic spatial resolution and whole-heart coverage, the T2 maps can be reformatted in any arbitrary plane. This advantage is best appreciated in Figure 7, where reformats in multiple standard orientations (short-axis, vertical long-axis, three-chamber and four-chamber) are shown for a healthy subject.

The need for using 2D iNAVs to correct for respiratory motion is shown in Supporting Information Figure S8, where the T2 maps of two healthy subjects are shown with and without 2D translational motion correction. Motion corrected T2 maps result in better visualization of the myocardium as compared to the non-motion-corrected T2 maps, which show some spatial blurring.

Patients

No cardiac findings were observed in the patient study. The acquisition times of the proposed 3D MUST-T2 sequence were 7 min 23 seconds (patient #1, mean heart rate: 75 bpm) and 8 min 43 seconds (patient #2, mean heart rate: 65 bpm). Figure 8 depicts the reconstructed apical, mid-cavity and basal T2 map slices, for the two patients, using the proposed 3D MUST-T2 framework compared with the current clinical reference maps (breath-held 2D T2p-SSFP). The proposed 3D MUST-T2 produces T2 maps with visual appearance comparable to the conventional 2D T2p-SSFP technique. Mean septal T2 relaxation times were similar between the two techniques (mid-ventricular slice: patient #1: 48.2 ± 4 ms 3D MUST-T2 versus 46.3 ± 3 ms 2D T2p-SSFP, and patient #2: 51.7 ± 7 ms 3D MUST-T2 versus 50.8 ± 4 ms 2D T2p-SSFP).

DISCUSSION

For Peer Review

In this study, we proposed a framework for highly accelerated free-breathing whole-heart T2 mapping that combines 2D translational respiratory motion correction, with a golden angle variable density spiral-like Cartesian trajectory and a recently introduced HD-PROST reconstruction. The proposed 3D MUST-T2 approach enables accurate and precise high-resolution isotropic (1.5mm^3) 3D whole-heart T2 mapping acquisitions in a fast and predictable scan time.

The performance of the proposed 3D T2 mapping framework was assessed in simulations, phantom experiments, and ten healthy subjects, while initial clinical feasibility was demonstrated in two patients with suspected cardiovascular disease.

3D MUST-T2 uses a saturation pulse to reset the magnetization immediately after the R-wave, as proposed by Ding et al. (17), and thus is mostly independent of heart rate variations. Another advantage of using saturation pulses compared to other T2 mapping techniques (3,5,16,31) is that recovery periods between subsequent heartbeats are not needed, thus reducing the total acquisition time.

Further acceleration through undersampling is crucial to achieve high isotropic resolution in a clinically feasible scan time. In phantom experiments, we observed that acceleration factors of up to 5-fold led to accurate T2 values ($R^2 > 0.99$) with respect to reference SE measurements. Besides the use of an efficient undersampling trajectory, the acquisition of low-resolution 2D iNAVs at every heartbeat also permits a substantial reduction in scan time by allowing 100% respiratory scan efficiency (no data rejection) and predictable scan time (24), as opposed to other respiratory-gated T2 mapping techniques based on dNAV acquisition (17). Other free-breathing T2 mapping techniques have been proposed to allow for 100% scan efficiency and predictable scan time. Van Heeswijk et al. (5) proposed a respiratory self-navigated 3D sequence to acquire isotropic 3D T2 maps with resolution of 1.7 mm^3 in a predictable scan time of ~18min at 3T, while Basha et al. (32) proposed a 2D multi-slice sequence with slice tracking. The significant scan time reduction achieved with 3D MUST-T2 was exploited to acquire in vivo isotropic whole-heart Cartesian T2 maps in clinically feasible scan times (~8 min), while a fully sampled acquisition would have

For Peer Review

required >35 mins. The total imaging time for 3D MUST-T2 being mainly affected by the subject's heart rate and the number of slices needed to cover the whole-heart in the anterior-posterior direction. For comparison, the conventional breath-hold 2D T2p-SSFP sequence would have required between 5 and 7 minutes to cover the entire heart (assuming 7 s breathing commands, 10 s resting time between acquisitions, 10 s breath-hold, and assuming that 11 to 16 slices are needed to cover the heart). The proposed 3D T2 mapping sequence can also be performed with lower anisotropic resolution (e.g., 2.0 x 2.0 x 6.0 mm^3 as achieved in (16)), that will result in shorter scan times and inherently co-registered slices due to the 3D nature of the acquisition.

The acquisition of undersampled data comes, however, at the cost of significant loss of information which needs to be recovered. Multi-contrast HD-PROST reconstruction takes advantage of the local, non-local and contrast redundancies found in the T2w images, to recover whole-heart T2 maps with negligible remaining aliasing artifacts. The measurements of myocardial T2 values by 3D MUST-T2 in healthy subjects (average septal T2 = 50.8 ± 3 ms) were in good agreement with in vivo values published in a previous study at 1.5T with centric ordering (T2 = 50 ± 4 ms (33)). T2 overestimation with respect to the conventional breath-hold 2D T2p-SSFP sequence was observed, with a bias of 4.2 ± 6.2 ms. This overestimation was likely due to the choice of centric (3D MUST-T2) versus linear (2D T2p-SSFP) k-space ordering, as observed by Giri et al. (3). Other confounding factors such as heart rate variations (34), not present in the phantom study, or the use of fat saturation and adiabatic T2 preparation pulses could also explain this overestimation in vivo and will be further explored.

Although high acceleration factors were reached with the proposed 3D sequence, precision of T2 values in vivo did not show significant deviations from the conventional 2D T2p-SSFP acquisitions (4.6 ± 1 ms vs. 4.3 ± 2 ms, $P = 0.520$), and were similar to previously reported values at 3T (5,17). This can be attributed to the good performance of HD-PROST reconstruction in concert with the VD-CASPR trajectory, which limits the propagation of noise in the T2w images, noise being a severe side effect of saturation-based MR mapping techniques (16,35,36).

For Peer Review

Dictionary-based matching was used in this study to accurately estimate myocardial T2 values by pre-generating a dictionary representative of the proposed T2 mapping sequence, and whose elements are composed of simulated signal evolution curves (28). Our findings in phantom experiments showed that dictionary-based matching has the potential to accurately estimate myocardial T2 values acquired with both 3D MUST-T2 and conventional T2p-bSSFP, whereas a T2 bias was observed with conventional mono-exponential fitting for both methods (Supporting Information Figure S4). This can be partly explained by the fact that mono-exponential fitting does not accurately describe the acquisition parameters and the signal evolution during acquisition, such as bSSFP T1/T2 ratio of tissue, subject-specific heart-rate, number of segments per heartbeat, and number of linear ramp-up pulses. Therefore, the use of dictionary-based matching could also improve conventional 2D T2p-SSFP and potentially reduce the bias observed with linear phase encoding.

A limitation of the current framework is that only 2D translation respiratory motion correction was performed to ensure fast reconstruction times. It has been shown in previous reports that non-rigid motion registration can improve reproducibility and spatial variability of 2D T2 mapping techniques (8,11). While this issue was not shown to be significant in the present experiments, it can be overcome by incorporating 3D non-rigid respiratory motion correction directly in the image reconstruction (37–39). Another alternative to deal with large motion between the T2w images is to extend the proposed HD-PROST reconstruction to enable motion-resolved reconstruction by extending the searching neighborhood for patch selection to the spatial-temporal dimension (40).

In this study, mid-diastolic imaging was employed to minimize cardiac motion and guarantee long saturation times. However, in subjects with highly variable heart rates or high heart rates, end-systolic imaging may be preferred. Future studies will investigate the effect of shorter saturation times on the accuracy and precision of saturation-based T2 mapping, however our phantom experiments demonstrate that accuracy is not affected for different heart rates between 50 and 100 bpm.

For Peer Review

Moreover, incomplete saturation of fat signal can occur in some regions of the T2w images, especially around the epicardial fat area. This effect can lead to fat-myocardium partial volume effect, apparent distortion and loss of sharpness on the T2 map and may alter the T2 measurements. Further optimized fat suppression for each T2w image will be investigated in the future to alleviate this difficulty.

Translational motion estimation and correction was performed inline in the scanner software while HD-PROST reconstruction and dictionary matching were performed offline. The efficient multithreaded implementation of HD-PROST allowed for fast T2 map reconstruction (in the order of 3 minutes). Further speedup, to reach sub-minute runtime, could be achieved by implementing the reconstruction on multiple GPUs and using coil compression strategies (41).

It should be noted that 3D MUST-T2 is based on a T2-prepared sequence commonly used in coronary MR angiography (42). The acceptable contrast provided by the last T2w volume (TE_{T2prep} = 55 ms, Figures 6 and 7) could also be exploited to visualize whole heart cardiac and proximal coronary artery anatomy. Thus, 3D MUST-T2 may be used for the simultaneous assessment of cardiac and coronary anatomy and myocardial T2 relaxation times in a highly simplified and efficient single free-breathing acquisition. This additional gain could potentially benefit patients with acute non-ST-segment elevation myocardial infarction where obstructive coronary artery disease and myocardial edema are often characteristic (13).

The proposed free-breathing T2 mapping framework could benefit many cardiovascular patients with severe shortness of breath and where imaging under breath-holding is often challenging. Preliminary insights into the potential of the proposed 3D MUST-T2 mapping technique in a clinical setting was provided for two patients with suspected cardiovascular disease. While no pathologies were observed in this proof-of-concept study, scanning patients often leads to new challenges (e.g., variable heart rate, irregular breathing pattern, poor compliance), resulting in degraded image quality. Higher amplitude in respiratory motion of the heart, as provided by the 2D iNAVs, was observed in patients compared to

For Peer Review

healthy controls (Supporting Information Figure S9). Mean septal T2 values measured on the two patients were comparable to that of the healthy subjects. Besides T2 relaxation times conform to the literature (Figure 8), the 3D whole-heart isotropic coverage of the proposed technique offers the opportunity to reformat the T2 maps in any desired orientation, which can be particularly useful for the comprehensive assessment of pathological tissues with complex geometry (6).

The proposed framework also shares similarities with the recent qBOOST-T2 approach (43) that enables co-registered bright-blood and black-blood whole-heart imaging, together with T2 quantification and coronary lumen visualization, through the use of an inversion pulse every three heartbeats. While the latest technique may be preferred whenever coronary assessment or pre-contrast black-blood images are clinically required, a thorough comparison of the two approaches in large patient cohorts will need to be studied.

Finally, the proposed fast and efficient framework holds promise for wider cardiac applications such as high-resolution motion compensated 3D T1 mapping and 3D joint T1-T2 mapping (44–49); both of which will be investigated in future works.

CONCLUSION

A novel approach was developed to enable free-breathing whole-heart 3D T2 mapping with high isotropic spatial resolution ($1.5mm^3$) in a clinically feasible scan time (<8 min with 100% scan efficiency and predictable scan time). The proposed 3D MUST-T2 framework achieved accurate T2 quantification in phantom and in vivo with fast acquisition. 3D-MUST T2 mapping may have potential to aid the management of many cardiomyopathies in which fast and efficient free-breathing acquisitions are key to patient comfort, while high isotropic resolution is crucial to accurately map tissue heterogeneity. Further studies to assess the clinical utility of 3D MUST-T2 mapping in patients with myocardial inflammation are now warranted.

ACKNOWLEDGMENTS

For Peer Review

EPG simulations were based on the algorithm described by Dr. Matthias Weigel in (19), made available on the author's website. The authors acknowledge financial support from EPSRC EP/P001009/, EP/P032311/1, EPSRC EP/P007619, Wellcome EPSRC Centre for Medical Engineering (NS/ A000049/1), and the Department of Health via the National Institute for Health Research (NIHR) comprehensive Biomedical Research Centre award to Guy's & St. Thomas' NHS Foundation Trust in partnership with King's College London and King's College Hospital NHS Foundation Trust. The views expressed are those of the authors and not necessarily those of the NHS, the NIHR, or the Department of Health.

ORCID

Aurelien Bustin https://orcid.org/0000-0002-2845-8617

Tevfik F. Ismail https://orcid.org/0000-0002-1691-7599

Claudia Prieto https://orcid.org/0000-0003-4602-2523

René M. Botnar https://orcid.org/0000-0003-2811-2509

For Peer Review

REFERENCES

1. Guo H, Au WY, Cheung JS, et al. Myocardial T2 quantitation in patients with iron overload at 3 Tesla. J. Magn. Reson. Imaging 2009;30:394–400 doi: 10.1002/jmri.21851.

2. He T, Gatehouse PD, Anderson LJ, et al. Development of a novel optimized breathhold technique for myocardial T2 measurement in thalassemia. J. Magn. Reson. Imaging 2006;24:580–5 doi: 10.1002/jmri.20681.

3. Giri S, Chung YC, Merchant A, et al. T2 quantification for improved detection of myocardial edema. J. Cardiovasc. Magn. Reson. 2009;11:1–13 doi: 10.1186/1532-429X-11-56.

4. Haberkorn SM, Spieker M, Jacoby C, Flögel U, Kelm M, Bönner F. State of the Art in Cardiovascular T2 Mapping: on the Way to a Cardiac Biomarker? Curr. Cardiovasc. Imaging Rep. 2018;11 doi: 10.1007/s12410-018-9455-3.

5. Van Heeswijk RB, Piccini D, Feliciano H, Hullin R, Schwitter J, Stuber M. Self-navigated isotropic three-dimensional cardiac T2 mapping. Magn. Reson. Med. 2015;73:1549–1554 doi: 10.1002/mrm.25258.

6. Ding H, Schar M, Zviman MM, Halperin HR, Beinart R, Herzka DA. High-resolution quantitative 3D T2 mapping allows quantification of changes in edema after myocardial infarction. J. Cardiovasc. Magn. Reson. 2013;15:345–347 doi: 10.1186/1532-429X-15-S1-P181.

7. Van Heeswijk RB, Piccini D, Tozzi P, et al. Three-dimensional self-navigated T2 mapping for the detection of acute cellular rejection after orthotopic heart transplantation. Transplant. Direct 2017;3 doi: 10.1097/TXD.0000000000000635.

8. Roujol S, Basha T, Weingartner S, et al. Motion correction for free breathing quantitative myocardial T2 mapping: impact on reproducibility and spatial variability. J. Cardiovasc. Magn. Reson. 2015;17:W5 doi: 10.1186/1532-429X-17-S1-W5.

For Peer Review

9. Jin N, Da Silveira JS, Jolly MP, et al. Free-breathing myocardial T2 mapping using GRE-EPI and automatic Non-rigid motion correction. J. Cardiovasc. Magn. Reson. 2015;17 doi: 10.1186/s12968-015-0216-z.

10. Odille F, Escanyé JM, Atkinson D, Bonnemains L, Felblinger J. Nonrigid registration improves MRI T2 quantification in heart transplant patient follow-up. J. Magn. Reson. Imaging 2015;42:168–174 doi: 10.1002/jmri.24741.

11. Giri S, Shah S, Xue H, et al. Myocardial T2 mapping with respiratory navigator and automatic nonrigid motion correction. Magn. Reson. Med. 2012;68:1570–1578 doi: 10.1002/mrm.24139.

12. Rauhalammi S, Layland J, Carrick D, et al. T1 and T2 Mapping Have Higher Diagnostic Accuracy for the Ischaemic Area-at-risk in Nstemi Patients Compared with Dark Blood Imaging. Heart 2014;100 doi: 10.3109/02699052.2014.892379.

13. Tessa C, Del Meglio J, Lilli A, et al. T1 and T2 mapping in the identification of acute myocardial injury in patients with NSTEMI. Radiol. Medica 2018;123:926–934 doi: 10.1007/s11547-018-0931-2.

14. Puntmann VO, Isted A, Hinojar R, Foote L, Carr-White G, Nagel E. T1 and T2 Mapping in Recognition of Early Cardiac Involvement in Systemic Sarcoidosis. Radiology 2017;285:63–72 doi: 10.1148/radiol.2017162732.

15. Van Heeswijk RB, Feliciano H, Bongard C, et al. Free-breathing 3T magnetic resonance T2-mapping of the heart. JACC Cardiovasc. Imaging 2012;5:1231–1239 doi: 10.1016/j.jcmg.2012.06.010.

16. Yang HJ, Sharif B, Pang J, et al. Free-breathing, motion-corrected, highly efficient whole heart T2 mapping at 3T with hybrid radial-cartesian trajectory. Magn. Reson. Med. 2016;75:126–36 doi: 10.1002/mrm.25576.

17. Ding H, Fernandez-De-Manuel L, Schär M, et al. Three-dimensional whole-heart T2 mapping at 3T. Magn. Reson. Med. 2015;74:803–816 doi: 10.1002/mrm.25458.

For Peer Review

18. Bustin A, Cruz G, Jaubert O, Lopez K, Botnar RM, Prieto C. High-dimensionality undersampled patch-based reconstruction (HD-PROST) for accelerated multi-contrast magnetic resonance imaging. Magn. Reson. Med. 2019;81:3705–3719 doi: 10.1002/mrm.27694.

19. Weigel M. Extended phase graphs: Dephasing, RF pulses, and echoes - Pure and simple. J. Magn. Reson. Imaging 2015;41:266–295 doi: 10.1002/jmri.24619.

20. Nezafat R, Stuber M, Ouwerkerk R, Gharib AM, Desai MY, Pettigrew RI. B1-insensitive T2 preparation for improved coronary magnetic resonance angiography at 3T. Magn. Reson. Med. 2006;55:858–64 doi: 10.1002/mrm.20835.

21. Prieto C, Doneva M, Usman M, et al. Highly efficient respiratory motion compensated free-breathing coronary MRA using golden-step Cartesian acquisition. J. Magn. Reson. Imaging 2015;41:738–746 doi: 10.1002/jmri.24602.

22. Bustin A, Ginami G, Cruz G, et al. Five-minute whole-heart coronary MRA with sub-millimeter isotropic resolution, 100% respiratory scan efficiency, and 3D-PROST reconstruction. Magn. Reson. Med. 2019;81:102–115 doi: 10.1002/mrm.27354.

23. Winkelmann S, Schaeffter T, Koehler T, Eggers H, Doessel O. An optimal radial profile order based on the golden ratio for time-resolved MRI. IEEE Trans. Med. Imaging 2007;26:68–76 doi: 10.1109/TMI.2006.885337.

24. Henningsson M, Koken P, Stehning C, Razavi R, Prieto C, Botnar RM. Whole-heart coronary MR angiography with 2D self-navigated image reconstruction. Magn. Reson. Med. 2012;67:437–445 doi: 10.1002/mrm.23027.

25. Ginami G, Neji R, Phinikaridou A, Whitaker J, Botnar RM, Prieto C. Simultaneous bright- and black-blood whole-heart MRI for noncontrast enhanced coronary lumen and thrombus visualization. Magn. Reson. Med. 2018;79:1460–1472 doi: 10.1002/mrm.26815.

26. Bustin A, Voilliot D, Menini A, et al. Isotropic Reconstruction of MR Images Using

For Peer Review

3D Patch-Based Self-Similarity Learning. IEEE Trans. Med. Imaging 2018;37:1932–1942 doi: 10.1109/TMI.2018.2807451.

27. Hennig J, Weigel M, Scheffler K. Calculation of flip angles for echo trains with predefined amplitudes with the extended phase graph (EPG)-algorithm: principles and applications to hyperecho and TRAPS sequences. Magn. Reson. Med. 2004;51:68–80 doi: 10.1002/mrm.10658.

28. Roccia E, Vidya Shankar R, Neji R, et al. Accelerated 3D T2 mapping with dictionary-based matching for prostate imaging. Magn. Reson. Med. 2019;81:1795–1805 doi: 10.1002/mrm.27540.

29. Captur G, Gatehouse P, Keenan KE, et al. A medical device-grade T1 and ECV phantom for global T1 mapping quality assurance - the T1 Mapping and ECV Standardization in cardiovascular magnetic resonance (T1MES) program. J. Cardiovasc. Magn. Reson. 2016;18:1–20 doi: 10.1186/s12968-016-0280-z.

30. Cerqueira MD, Weissman NJ, Dilsizian V, et al. Standardized myocardial segmentation and nomenclature for tomographic imaging of the heart: a statement for healthcare professionals from the cardiac imaging. Circulation 2002;105 doi: 10.1161/hc0402.102975.

31. Darçot E, Yerly J, Colotti R, et al. Accelerated and high-resolution cardiac T2 mapping through peripheral k-space sharing. Magn. Reson. Med. 2019;81:220–233 doi: 10.1002/mrm.27374.

32. Basha TA, Bellm S, Roujol S, Kato S, Nezafat R. Free-breathing slice-interleaved myocardial T2 mapping with slice-selective T2 magnetization preparation. Magn. Reson. Med. 2016;76:555–565 doi: 10.1002/mrm.25907.

33. Blume U, Lockie T, Stehning C, et al. Interleaved T1 and T2 relaxation time mapping for cardiac applications. J. Magn. Reson. Imaging 2009;29:480–487 doi: 10.1002/jmri.21652.

For Peer Review

34. Granitz M, Motloch LJ, Granitz C, et al. Comparison of native myocardial T1 and T2 mapping at 1.5T and 3T in healthy volunteers: Reference values and clinical implications. Wien. Klin. Wochenschr. 2019;131:143–155 doi: 10.1007/s00508-018-1411-3.

35. Nordio G, Bustin A, Henningsson M, et al. 3D SASHA myocardial T1 mapping with high accuracy and improved precision. Magn. Reson. Mater. Physics, Biol. Med. 2018 doi: 10.1007/s10334-018-0703-y.

36. Bustin A, Ferry P, Codreanu A, et al. Impact of denoising on precision and accuracy of saturation-recovery-based myocardial T1 mapping. J. Magn. Reson. Imaging 2017;46:1377–1388 doi: 10.1002/jmri.25684.

37. Odille F, Menini A, Escanye J-M, et al. Joint reconstruction of multiple images and motion in MRI: application to free-breathing myocardial T2 quantification. IEEE Trans. Med. Imaging 2016;35:197–207 doi: 10.1109/TMI.2015.2463088.

38. Batchelor PG, Atkinson D, Irarrazaval P, Hill DLG, Hajnal J, Larkman D. Matrix description of general motion correction applied to multishot images. Magn. Reson. Med. 2005;54:1273–1280 doi: 10.1002/mrm.20656.

39. Cruz G, Atkinson D, Henningsson M, Botnar RM, Prieto C. Highly efficient nonrigid motion-corrected 3D whole-heart coronary vessel wall imaging. Magn. Reson. Med. 2017;77:1894–1908 doi: 10.1002/mrm.26274.

40. Kuestner T, Bustin A, Cruz G, et al. 3D Cartesian free-running cardiac and respiratory resolved whole-heart MRI. In: Proceedings of the 27th Annual Meeting of ISMRM Montreal Canada. ; 2019. p. 2192.

41. Zhang T, Pauly JM, Vasanawala SS, Lustig M. Coil compression for accelerated imaging with Cartesian sampling. Magn. Reson. Med. 2013;69:571–82 doi: 10.1002/mrm.24267.

42. Botnar RM, Stuber M, Danias PG, Kissinger K V, Manning WJ. Improved coronary

For Peer Review

artery definition with T2-weighted, free-breathing, three-dimensional coronary MRA. Circulation 1999;99:3139–3148 doi: 10.1161/01.CIR.99.24.3139.

43. Milotta G, Ginami G, Bustin A, Neji R, Prieto C, Botnar RM. 3D whole-heart free-breathing BOOST-T2 mapping. In: Proceedings of the 27th Annual Meeting of ISMRM Montreal Canada. ; 2019. p. 2002.

44. Akçakaya M, Weingärtner S, Basha TA, Roujol S, Bellm S, Nezafat R. Joint myocardial T1 and T2 mapping using a combination of saturation recovery and T2-preparation. Magn. Reson. Med. 2016;76:888–896 doi: 10.1002/mrm.25975.

45. Kvernby S, Warntjes MJ an B, Haraldsson H, Carlhäll CJ, Engvall J, Ebbers T. Simultaneous three-dimensional myocardial T1 and T2 mapping in one breath hold with 3D-QALAS. J. Cardiovasc. Magn. Reson. 2014;16:102 doi: 10.1186/s12968-014-0102-0.

46. Xanthis CG, Bidhult S, Greiser A, et al. Simulation-based quantification of native T1 and T2 of the myocardium using a modified MOLLI scheme and the importance of Magnetization Transfer. Magn. Reson. Imaging 2018;48:96–106 doi: 10.1016/j.mri.2017.12.020.

47. Guo R, Chen Z, Herzka DA, Luo J, Ding H. A three-dimensional free-breathing sequence for simultaneous myocardial T1 and T2 mapping. Magn. Reson. Med. 2018:1031–1043 doi: 10.1002/mrm.27466.

48. Santini F, Kawel-Boehm N, Greiser A, Bremerich J, Bieri O. Simultaneous T1 and T2 quantification of the myocardium using cardiac balanced-SSFP inversion recovery with interleaved sampling acquisition (CABIRIA). Magn. Reson. Med. 2015;74:365–371 doi: 10.1002/mrm.25402.

49. Milotta G, Ginami G, Bustin A, Neji R, Prieto C, Botnar RM. 3D Whole-heart High-resolution Motion Compensated Joint T1/T2 Mapping. In: Proceedings of the 27th Annual Meeting of ISMRM Montreal Canada. ; 2019. p. 2003.

For Peer Review

Figure Captions

Figure 1 Schematic overview of the proposed free-breathing 3D MUST-T2 technique for whole-heart myocardial T2 mapping. Three T2-prepared volumes are acquired sequentially with increasing TE_{T2prep} ([0,28,55] ms). A nonselective saturation pulse is applied immediately after the ECG R-wave to avoid recovery heartbeats. A 2D image-navigator is acquired to enable translational respiratory motion correction of the heart and shorter and predictable scan times. A golden-angle shifted variable density Cartesian undersampling is employed to achieve clinically feasible scan times. All T2 prepared volumes are reconstructed simultaneously with HD-PROST (18). A dictionary is then simulated and matched to the measured signal to generate the whole-heart T2 maps. Abbreviations: TD, trigger delay; T_{SAT}, saturation time; AW, acquisition window

Figure 2 Results from EPG simulations show the effect of the saturation pulse on the MR signal evolution. (A) shows the simulated magnetization obtained with the EPG formalism for different recovery times (ranging from 0 to 9 seconds) when the saturation pulse is not used. The signals were generated for tissues with a T2 of 50 ms, varying T1s (ranging from 700 ms to 1200 ms), TE_{T2prep} = 50 ms, and a simulated heart rate of 60 bpm. For long T1s, a minimum of ~6 idle heartbeats are needed to allow for full recovery of the longitudinal magnetization. When the saturation pulse is applied at every heartbeat (B), idle heartbeats are not required for signal recovery, at the cost of lower signal intensity. (C) Evolution of the matched T2 values obtained with the proposed 3D MUST-T2 mapping sequence over different simulated heart rates (ranging from 50 bpm to 100 bpm) for each phantom vial. The proposed approach is mostly insensitive to heart rate variations, even for long T1s. (D) The effect of different heart rates across all healthy subjects (N = 10) on mean T2 values is shown.

Figure 3 Phantom accuracy for the proposed 3D MUST-T2 sequence. Plots are comparing the mean T2 values derived from the nine vials for five different acceleration factors with the ground truth T2 values (measured by SE with eight TEs from 10-640 ms (29)), conventional 2D T2p-SSFP mapping (green) and the proposed 3D MUST-T2 sequence. T2

For Peer Review

accuracy is preserved with the proposed approach with excellent agreement with the reference T2 values, even for high acceleration (x5). T2 values for the last tube (T2 = 250ms) were out of range (>300 ms) for the 2D T2p-SSFP sequence and therefore are not shown.

Figure 4 T2 maps obtained using the proposed free-breathing 3D MUST-T2 sequence and the conventional breath-held 2D T2p-SSFP sequence are shown for three healthy subjects. 3D MUST-T2 slices were reformatted to short-axis to match the 2D T2 map acquisitions. Good visualization of the myocardium and surrounding structures can be observed on the 3D MUST-T2 maps. Acquisition times are expressed as [min:sec]. Abbreviations: BPM, beats per minute; AT, acquisition time

Figure 5 Accuracy and precision of the proposed 3D MUST-T2 mapping sequence. (A) T2 accuracy of the proposed 3D MUST-T2 sequence versus conventional 2D T2p-SSFP, as measured by the mean T2 value are shown in the left ventricular segmentation. T2 values are in good agreement with the literature (T2 = 50 ± 4 ms (33)). The averaged T2 relaxation times over the whole myocardium are shown in the bull's eye plots' center. Accuracy (B) and precision (C) of T2 relaxation times (ms) obtained in the myocardial septum with the proposed 3D MUST-T2 and the conventional 2D T2p-SSFP are shown for the 10 healthy subjects.

Figure 6 Three-dimensional visualization of the acquired T2w images and the corresponding T2 volume. Representative T2w images for subject 2 (acquisition time: 10 min, heart rate = 38 bpm), and the corresponding T2 maps obtained by the proposed 3D MUST-T2. Eight reformatted short-axis slices that cover the heart from apex to base are shown. Uniform distribution of T2 values through the slices over the whole-left ventricle can be observed. The color scale indicates T2 values between 0-120 ms.

Figure 7 Representative T2-prepared images for subject 2 and the corresponding T2 maps obtained with the proposed 3D MUST-T2 sequence. Reformats in short-axis, vertical long-axis, 3-chamber and 4-chamber views are shown.

For Peer Review

Figure 8 Short-axis T2 maps at apical, mid-ventricular and basal level for two patients acquired with the proposed free-breathing 3D MUST-T2 framework and the conventional breath-hold 2D T2p-SSFP sequence. The septal T2 relaxation times for each slice are reported as mean ± standard deviation.

Supporting Information Figure Captions

Additional Supporting Information may be found in the online version of this article.

Supporting Information Figure S1 A 3D Cartesian variable-density trajectory was employed to allow for fast acquisition of multiple T2w images. The Cartesian trajectory with spiral order samples the k_y-k_z phase encoding plane following approximate spiral interleaves on the Cartesian grid with variable density along each spiral arm. In this sketch, the 2 first acquired spirals are shown for each contrast, each spiral containing 20 segments. A golden angle rotation between successive spirals and successive contrasts is applied to introduce incoherently distributed aliasing artifacts along the contrast dimension, and noise-like artifacts in the spatial dimension.

Supporting Information Figure S2 Flowchart of the optimization 2 of the proposed High-Dimensionality Patch-based RecOnSTruction (HD-PROST). Denoising of multiple T2w images is performed using a 3D block matching, which groups and unfolds similar 3D patches in the noisy multi-contrast images to form a low-rank 2D matrix. A third-order tensor is formed by stacking the T2 contrast dimension on the third dimension. The high-order tensor of size N (number of pixels in each patch) x K (number of similar patches within a neighborhood) x L (number of T2 contrasts) admits a low multilinear rank approximation and can be compressed, through high-order tensor decomposition, by truncating the multilinear singular vectors that correspond to small multilinear singular values. The outputs of this step are the denoised multi-contrast images which are then used in the joint regularized reconstruction step (optimization 1) as prior knowledge. Reconstruction parameters used in this study are shown (bottom row). We refer the reader to (18) for more information on these parameters. Reconstruction parameter details: N,

For Peer Review

patch size (in pixels); L, number of contrasts; K, number of similar patches; λ_p, threshold value.

Supporting Information Figure S3 Simulations of the proposed T2 mapping sequence were performed using the EPG formalism to assess the effect of T1 in the EPG-based dictionary on the matched T2 value. Signals evolutions for different T1 (from 850 to 1200 with a step size of 50 ms) and T2 (from 42 to 82 with a step size of 8 ms) were generated and matched to a dictionary simulated with fixed T1 (1100 ms) and varying T2s (similar to the one used in the phantom experiment). (A) Matched T2 is plotted as a function of T1. (B) The signal evolutions corresponding to short (T1/T2 = 800/52 ms), medium (T1/T2 = 1100/52 ms), and long (T1/T2 = 1300/52 ms) T1 myocardium were generated for the proposed sequence through EPG simulation. The obtained signal evolutions did not seem to differ, suggesting that the proposed 3D MUST-T2 map sequence with dictionary-based matching is independent of the T1 used in the EPG-based dictionary (matched T2s were the same for the three generated signals and equal to 52 ms). Therefore, for the phantom and in vivo experiments, we kept the T1 constant at 1100 ms.

Supporting Information Figure S4 Conventional mono-exponential fitting and dictionary-based matching for 2D T2p-SSFP T2 mapping in comparison to the proposed 3D MUST-T2 sequence for the phantom study. The proposed 3D acquisition with mono-exponential fitting is also included for comparison purposes. Accurate phantom T2 values, in agreement with reference spin echo, were obtained with the proposed 3D MUST-T2 sequence with dictionary-based matching, however bias is observed with the proposed acquisition when mono-exponential fitting is employed. Bias is also observed with the conventional (linear phase encoding) 2D T2p-SSFP mapping with mono-exponential fitting, however this bias is significantly reduced when dictionary-based matching is employed.

Supporting Information Figure S5 Spatial T2 uniformity over the slice direction is assessed for the phantom study for three vials (corresponding to short, medium and long T1 myocardium). The solid line is the average difference between gold-standard spin echo

For Peer Review

and the proposed 3D MUST-T2 mapping sequence, and the dashed lines represent the mean ± two standard deviations between the two techniques. Good T2 uniformity can be observed with the proposed technique. The mean difference in T2 for the vial corresponding to short T1 myocardium was -0.6 ms [±95% confidence interval (CI) = -2.1/0.89 ms), -0.6 ms [±95% CI = -3.7/2.5 ms) for the medium T1 myocardium, and -1.4 ms [±95% CI = -4.9/2.0 ms) for the long T1 myocardium.

Supporting Information Figure S6 T2 maps obtained using the proposed free-breathing 3D MUST-T2 mapping sequence and the conventional breath-held 2D T2p-SSFP sequence are shown for three additional healthy subjects. 3D MUST-T2 slices were reformatted to short-axis to match the 2D T2 map acquisitions. Representative 16 AHA segments are shown to illustrate how much spatial information was considered for T2 calculation. Acquisition times are expressed as [min:sec]. Abbreviations: BPM, beats per minute; AT, acquisition time.

Supporting Information Figure S7 Axial view of T2 maps acquired using the proposed 3D T2 mapping sequence on 3 healthy subjects. Number of slices was adjusted per subject to cover the left ventricle in the anterior-posterior direction.

Supporting Information Figure S8 Impact of iNAV-based beat-to-beat translation motion correction on 3D MUST-T2 map is shown for two healthy subjects. Reconstructed T2w images (TE_{T2prep} = 55 ms) are shown before and after motion correction with the corresponding T2 maps (A). Better visualization of the myocardium can be observed after motion correction with clear delineation of cardiac structures and myocardial walls. Note the blurring observed on the non-motion corrected T2 maps. Plots showing the intensity profiles, taken on the T2w images through the heart-liver interface, are shown in (B).

Supporting Information Figure S9 (A) Foot-head respiratory displacements of the heart obtained from the 2D image navigators at each heartbeat are shown for 2 representative healthy subjects (left) and 2 patients (right). The end-expiration position is used as reference for translational motion estimation. While regular breathing patterns can be observed on the healthy subjects, more irregular breathing patterns with strong motion amplitudes are

For Peer Review

observed on patient 1 and patient 2. (B) Average R-R intervals are shown for each healthy subject and patient. Patient 1 presented with irregular cardiac rhythm (R-R = 838±211 ms).

For Peer Review

Accelerated Free-Breathing Whole-Heart 3D T2 Mapping with High Isotropic Resolution

Aurélien Bustin[1], Giorgia Milotta[1], Tevfik F. Ismail[1], Radhouene Neji[1,2], René M. Botnar[1,3], Claudia Prieto[1,3]

[1]Department of Biomedical Engineering, School of Biomedical Engineering and Imaging Sciences, King's College London, London, United Kingdom
[2]MR Research Collaborations, Siemens Healthcare Limited, Frimley, United Kingdom
[3]Escuela de Ingeniería, Pontificia Universidad Católica de Chile, Santiago, Chile

For Peer Review

Short Title: Free-Breathing Whole-Heart 3D T_2 Mapping
Submitted as Full Paper to Journal of Magnetic Resonance in Medicine
Main document word count: 5140

Corresponding author:

Name Aurélien Bustin, PhD
School of Biomedical Engineering and Imaging Sciences
King's Health Partners, King's College London
Address 3rd Floor, Lambeth Wing, St Thomas' Hospital
London SE1 7EH
United Kingdom
E-mail aurelien.bustin@kcl.ac.uk

ABSTRACT

Purpose: To enable free-breathing whole-heart 3D T2 mapping with high isotropic resolution in a clinically feasible and predictable scan time. This 3D Motion-corrected Undersampled Signal maTched (MUST)-T2 map is achieved by combining an undersampled motion-compensated T2-prepared Cartesian acquisition with a high-order patch-based reconstruction.

Methods: 3D MUST-T2 mapping acquisition consists of an ECG-triggered, T2-prepared, balanced steady-state free precession sequence with non-selective saturation pulses. Three undersampled T2-weighted volumes are acquired using a 3D Cartesian variable-density sampling with increasing T2 preparation times. A 2D image-based navigator is used to correct for respiratory motion of the heart and allow 100% scan efficiency. Multi-contrast HD-PROST reconstruction is used in concert with dictionary matching to generate 3D T2 maps. The proposed framework was evaluated in simulations, phantom experiments, and in vivo (10 healthy subjects, 2 patients) with 1.5mm^3 isotropic resolution. 3D MUST-T2 was compared against standard multi-echo spin-echo sequence (phantom) and conventional breath-held single-shot 2D SSFP T2 mapping (in-vivo).

Results: 3D MUST-T2 showed high accuracy in phantom experiments (R^2>0.99). The precision of T2 values was similar for 3D MUST-T2 and 2D bSSFP T2 mapping in-vivo (5±1ms vs. 4±2ms, *P*=0.52). Slightly longer T2 values were observed with 3D MUST-T2 in comparison to 2D bSSFP T2 mapping (50.7±2ms vs. 48.2±1ms, P<0.05). Preliminary results in patients demonstrated T2 values in agreement with literature values.

Conclusion: The proposed approach enables free-breathing whole-heart 3D T2 mapping with high isotropic resolution in ~8 min, achieving accurate and precise T2 quantification of myocardial tissue in a clinically feasible scan time.

Keywords: myocardial T2 mapping, T2 quantification, fast imaging, motion correction, isotropic resolution

For Peer Review

INTRODUCTION

Quantitative myocardial T2 mapping has emerged as a promising tool for edema characterization and detection of subtle myocardial inflammation in patients with acute myocardial infarction, myocarditis, dilated cardiomyopathy, sarcoidosis, and autoimmune cardiomyopathies (1–4).

Myocardial T2 mapping is usually performed by acquiring several ECG-triggered T2-weighted (T2w) images, with different amounts of T2 decay through T2-preparation pulses. A map of T2 relaxation times is then generated by fitting the series of weighted images to an exponential decay model on a pixel-by-pixel basis. Current clinical protocols usually perform myocardial T2 mapping with a two-dimensional (2D) single-shot steady-state free-precession sequence (T2p-SSFP), acquiring three T2-prepared images in a single-breathold every two to three heartbeats to allow for full T1 recovery (3). Multiple short-axis slices are usually acquired at the basal, mid-ventricular and apical level.

However, the use of 2D acquisitions with fairly thick slices and the associated partial volume effects undermine the full potential of myocardial T2 mapping, particularly in hypertrophic cardiomyopathies where the pathological tissues are often complex three-dimensional structures with differing T2 values (5–7). Furthermore, 2D sequences, typically acquired during breath holding, regularly suffer from respiratory and cardiac motion between the T2w images, mainly due to imperfect breath-holding or variable heart rate (8). Although robust non-rigid motion-correction techniques have been proposed to correct for residual motion and improve map quality, such techniques are relatively complex, computationally expensive and only correct for in-plane motion (9–11).

A free-breathing 3D T2 mapping approach with high isotropic spatial resolution may have the potential to increase diagnostic accuracy in patients with acute myocardial injury (e.g., NSTEMI patients (12,13)), and improve the detection of cardiac involvement in patients with systemic sarcoidosis (14).

For Peer Review

Three-dimensional (3D) myocardial T2 mapping techniques have been proposed to address the limitations of 2D imaging by allowing for large coverage of the heart with inherently higher signal-to-noise ratio (SNR). Non-cartesian self-navigated myocardial T2 mapping has been proposed to perform free-breathing 3D myocardial T2 mapping at 3T in ~18 min acquisition time (5,15). Such long scan times, unfortunately, may impede the clinical integration of this technique. A self-navigated hybrid radial-cartesian trajectory was also proposed to perform free-breathing 3D myocardial T2 mapping in less than 5 min, however with low spatial resolution (16). The use of saturation pulses at every heartbeat was proposed to accelerate Cartesian 3D T2 mapping (17). Long resting periods (in the order of 2-3 heartbeats (3,5) are usually needed in T2 mapping to ensure full recovery of the longitudinal magnetization between acquisitions to minimize T1 effects and satisfy the assumption that the equilibrium state magnetization is not affected by heart rate variations throughout the scan. Non-selective 90° saturation pulses reset magnetization history by tipping the longitudinal magnetization of the imaged volume into the transverse plane, thus removing heart rate dependency during the acquisition and allowing for imaging every heartbeat. This approach also eliminates artifacts caused by heart rate variations, at the cost of a reduced SNR and lower precision of T2 values. However, this technique uses prospective diaphragmatic navigator-gated (dNAV) acquisitions and thus leads to prolonged and often unpredictable scan times (~9 min nominal scan time with 30% to 60% respiratory gating efficiency) since only a small fraction of the acquired data is accepted for reconstruction (referred to as low scan efficiency).

Notwithstanding the continued advancements, myocardial 3D T2 mapping still faces substantial technical challenges which in turn may limit its applicability in clinical practice. In this study, we sought to achieve high isotropic spatial resolution 3D Cartesian whole-heart myocardial T2 mapping in a short and predictable scan time of ~8 min by combining a highly accelerated saturation-based free-breathing myocardial T2 mapping sequence with 2D image-based navigator (iNAV) based respiratory motion correction. A recently proposed high-dimensionality undersampled patch-based reconstruction (HD-PROST) (18) is employed in concert with dictionary matching, based on the Extended Phase Graph

For Peer Review

(EPG) formalism (19), to allow for accurate and precise myocardial T2 maps ~~with good image quality.~~ The proposed framework was validated in simulations, phantom and healthy subject experiments, while its initial clinical feasibility was shown for two patients with suspected cardiovascular disease.

Commented [BA1]: R2.1

METHODS

Acquisitions were performed on a 1.5T MR scanner (Magnetom Aera, Siemens Healthcare, Erlangen, Germany) with a dedicated 18-channel body coil and a 32-channel spine coil. Written informed consent was obtained from all healthy subjects and patients before undergoing MRI scans and the study was approved by the National Research Ethics Service. Numerical simulations, reconstructions and analysis were performed on a workstation with a 16-core Dual Intel Xeon Processor (2.3 GHz, 256GB RAM).

Accelerated Whole-heart 3D T2 Mapping Sequence

The proposed myocardial 3D Motion corrected Undersampled Signal maTched (MUST)-T2 mapping sequence is shown in Figure 1. A saturation pulse is performed right after the R-wave with a constant T_{SAT} time from the data acquisition. T_{SAT} is set to the maximal available time allowed by the sequence to guarantee enough magnetization recovery before the next acquisition. This approach allows efficient imaging at every heartbeat, avoiding the use of multiple recovery periods (17). Subsequently, an adiabatic T2 prepared pulse with variable echo time (TE_{T2prep}) is performed, followed by a balanced steady-state free-precession (bSSFP) read-out. An adiabatic T2-prep module (Silver-Hoult type) is employed due its good insensitivity to B1 and B0 inhomogeneities (20). Three T2w volumes are acquired sequentially with different T2-weightings (TE_{T2prep} = [0, 28, 55] ms).

A 3D Cartesian variable-density trajectory with spiral profile order (VD-CASPR) (21,22) is employed to allow for fast acquisition of the three T2-prepared volumes. This trajectory samples the k_y-k_z phase-encoding plane following approximate spiral interleaves on the Cartesian grid with variable density along each spiral arm and with two successive spiral interleaves being rotated by the golden angle. A golden angle rotation (21,23) between

For Peer Review

different contrast acquisitions was incorporated to introduce incoherently distributed aliasing along the contrast dimension and noise-like artifacts in the spatial dimension (Supporting Information Figure S1).

A 2D low-resolution iNAV (24) precedes the 3D acquisition at every heartbeat to enable 2D translational respiratory motion estimation/compensation (superior-inferior and right-left directions). This technique, already validated for coronary MR angiography (24) and multi-contrast cardiac MRI (25), enables 100% scan efficiency with predictable scan time, resulting in ~2-3 times acceleration compared to dNAV-based acquisitions. 2D iNAVs are obtained by spatially encoding the startup echoes of the bSSFP T2 mapping sequence. 2D translational motion is estimated using a template-matching algorithm with normalized cross-correlation as similarity measure, with the template manually selected around the heart during acquisition planning. Motion compensation of the three volumes is performed by modulating the k-space data with a linear phase shift to a reference respiratory position selected at end-expiration (24).

Multi-Contrast HD-PROST Reconstruction

Multi-contrast HD-PROST (18,22) is employed to reconstruct the three undersampled T2w volumes. HD-PROST exploits local (i.e., within a patch), non-local (i.e., between similar patches within a neighborhood) and contrast (i.e., between T2w images) redundancies of the 3D volumes in an efficient low-rank formulation. The reconstruction is formulated as an iterative two-step process: 1) an L2-norm regularized parallel-imaging reconstruction using the denoised multi-contrast data from step 2 as a prior (optimization 1), and 2) an efficient high-order low-rank patch-based denoising (optimization 2, Supporting Information Figure S2). The first step is optimized by gradient descent, whereas the second step is optimized through high-order low-rank tensor decomposition. The performance of HD-PROST reconstruction relies mainly on two parameters that need to be carefully tuned in order to get the best reconstruction quality: i) the patch size ($N = 5 \times 5 \times 5$ pixels in this study), reflecting the degree of structural information within each patch; and ii) the high-

For Peer Review

order singular value truncation parameter ($\lambda_p = 0.1$ in this study) which controls the amount of regularization.

HD-PROST reconstruction was implemented and performed offline using the algorithm described in (18). Reconstruction parameters were empirically optimized (as previously reported) and are illustrated in Supporting Information Figure S2. We refer the reader to (18,26) for a detailed description of HD-PROST and the associated reconstruction parameters.

Numerical Simulations

Usually in myocardial T2 mapping, the acquisition of each T2-weighted image is followed by a resting period of ~2-3 heartbeats to allow for full longitudinal magnetization relaxation. Numerical EPG simulations were first performed to investigate the impact of removing recovery heartbeats, and integrating saturation pulses, on the longitudinal magnetization of 3D MUST-T2 for tissues with different relaxation times T1. Simulations were performed for a T2 of 50 ms and varying T1 values (ranging from 700 ms to 1200 ms) with and without saturation pulses. Other relevant parameters used in the simulations were TE_{T2prep} = 55 ms, repetition time (TR) = 3.2 ms, trigger delay = 856 ms, data-acquisition window of 100 ms, and a simulated heart rate of 60 beats per minute (bpm).

Dictionary Generation and Matching

3D MUST-T2 dictionaries are simulated using the EPG formalism (19,27,28) for a range of T2 values. For both phantom and in vivo experiments, the dictionaries are calculated matching the subject-specific acquisition parameters with T2s in the range [minimum: step size: maximum] of [4:2:100, 105:5:200, 210:10:450] ms. Simulations show that the proposed method is not dependent on the used T1 value (in the range of interest) for dictionary generation (Supporting Information Figure S3, where the simulation results are shown for different T1 values ranging from 850 ms to 1200 ms with a step size of 50 ms), thus T1 is kept constant at 1100 ms for the phantom and in-vivo experiments. T2 maps are obtained by voxel-wise matching of the measured and normalized signal to the closest

For Peer Review

(minimum least square) EPG-based dictionary entry. The choice of dictionary-based matching versus conventional mono-exponential curve fitting is justified in Supporting Information Figure S4.

Phantom Experiments

The proposed ECG-triggered 3D MUST-T2 mapping sequence was evaluated in a standardized (T1MES) T1/T2 phantom containing nine agarose-based tubes with relevant cardiac T1 and T2 combinations (range, T1: 255 ms to 1489 ms, T2: 44 ms to 243 ms) (29). Scan parameters for 3D MUST-T2 included: TR = 3.13 ms, echo time (TE) = 1.37 ms, flip angle (FA) = 90°, field-of-view (FOV) = 187x187x156 mm^3, 1.5 mm^3 isotropic resolution, bandwidth (BW) = 908 Hz/pixel, data-acquisition window = 100 ms, TE_{T2prep} = [0, 28, 55] ms. Reference T2 relaxation times for each vial were obtained using a multi-echo spin-echo (SE) sequence with eight TEs ranging from 10 ms to 640 ms. In addition, conventional ECG-triggered 2D T2p-SSFP was performed for comparison purposes with the following imaging parameters: 1.9 x 1.9 mm^2 in-plane resolution, slice thickness = 8 mm, TR/TE = 3.11/1.38 ms, linear k-space reordering, BW = 1184 Hz/pixel, TE_{T2prep} = [0, 25, 55] ms, FA = 70°, 3 recovery beats, GRAPPA factor 2 with 36 k-space auto-calibration lines. The T2 relaxation times were obtained by mono-exponential curve fitting for both SE and T2p-SSFP sequences.

Impact of heart rate on T2 accuracy

The impact of heart rate differences on T2 accuracy was assessed by performing multiple 3D MUST-T2 phantom acquisitions with different simulated heart rates (ranging from 50 bpm to 100 bpm, step size 10 bpm). The trigger delay was set to 70% of the R-R interval and ranged from 420 ms to 840 ms, while the saturation time T_{SAT} was always set to the maximum allowed time (ranging from 370 ms to 790 ms). The acquisitions were performed fully sampled using the previously described VD-CASPR sampling.

Impact of acceleration on T2 accuracy

For Peer Review

To study the impact of accelerating 3D MUST-T2 on the accuracy of the T2 values, several phantom acquisitions were performed with different undersampling factors ranging from 1-fold to 5-fold (step size 1). Additional acquisition parameters included: simulated heart rate of 60 bpm, trigger delay of 680 ms, and saturation time T_{SAT} = 630 ms.

Data Analysis

Circular regions of interest were drawn on each vial for 3D MUST-T2, SE and 2D T2p-SSFP sequences. For each vial, the average T2 value was measured and agreement between SE, 2D T2p-SSFP T2 values and the proposed approach was assessed using linear regression.

In Vivo Experiments

Healthy Subjects

Ten healthy subjects (5 men and 5 women, mean age: 30-year-old, range: 26-36 years) with no history of cardiovascular disease underwent ECG-triggered free-breathing 3D whole-heart T2 mapping using the proposed 3D MUST-T2 acquisition approach. Relevant scan parameters included: FOV = 320 x 320 x 84-108 mm^3, slice-oversampling 22%, 1.5 mm^3 isotropic resolution, FA = 90°, TE_{T2prep} = [0, 28, 55] ms, subject-dependent mid-diastolic trigger delay (mean: 672 ms, range: 521-952 ms), acquisition window (mean: 97 ms, range: 80-108 ms), T_{SAT} (range: 470-900 ms), acceleration factor of 5x, 14 linear ramp-up pulses for iNAV, and Hanning-filtered sinc pulse with a duration of 1 ms and time-bandwidth product of 4.5. To ensure adequate fat suppression, a spectral pre-saturation with inversion recovery (SPIR) was applied before imaging. All 3D MUST-T2 mapping acquisitions were performed in the coronal plane.

Conventional 2D T2p-SSFP T2 mapping (3) was acquired for each subject for comparison purposes. Acquisition parameters were the same as for the phantom experiments. Three short-axis slices (basal, mid-cavity, apical) were acquired in three separate breath-holds of ~10 seconds each. A non-rigid motion correction was carried out inline to compensate for

For Peer Review

in-plane motion between the three 2D T2w images (11). Subsequently, T2 maps were obtained by mono-exponential curve fitting.

Patients

The feasibility and preliminary clinical performance of the proposed 3D MUST-T2 sequence was assessed in two patients (2 men, age: 42-year-old and 50-year-old) with suspected cardiovascular disease. The same acquisition and reconstruction parameters as in the healthy subject study were used. The patient-specific saturation times were T_{SAT} = 525 ms (patient #1, average heart rate: 75 bpm, acquisition window = 98 ms) and T_{SAT} = 595 ms (patient #2, average heart rate: 65 bpm, acquisition window = 100 ms). Conventional 2D T2p-SSFP T2 mapping was acquired for each patient with same parameters as in the healthy subject study.

Data Analysis

3D MUST-T2 maps were reformatted in the short-axis view to match the 2D T2p-SSFP slices. Regional differences in left ventricular T2 relaxation times were assessed according to the 16-segment model of the American Heart Association (AHA) (30). T2 measurements were reported as mean ± standard deviation and assessed using Student's t-test. Statistical differences in regional T2 values among reformatted basal, mid-ventricular and apical short-axis slices were analyzed using repeated-measures one-way analysis of variance (ANOVA) with Bonferroni post-hoc comparisons. All statistical analyses were performed using MATLAB (v7.1, The MathWorks, Natick, MA), and statistical significances were defined as a P value < 0.05.

RESULTS

Numerical Simulations

The impact of recovery times on the signal intensity (longitudinal magnetization) is depicted in Figure 2a-b for multiple T1 relaxation times (ranging from 700 ms to 1200 ms). While a clear dependency was observed when no saturation pulse is applied, necessitating

For Peer Review

~2-3 resting periods to recover 96% of the signal intensity (Figure 2a), applying a 'reset' saturation pulse (17) at every heartbeat avoids recovery periods, at the cost of a lower signal intensity (Figure 2b).

Phantom Experiments

Average T2 values obtained in the phantom experiments when increasing the simulated heart rate (from 50 bpm to 100 bpm) are depicted in Figure 2c. T2 relaxation times measured with the proposed 3D MUST-T2 sequence showed no to little sensitivity to change of heart rate for all vials in comparison to SE reference measurements.

Accuracy of the T2 values obtained with the proposed 3D MUST-T2 approach in phantom is shown in Figure 3 for different acceleration factors. Excellent linear correlation was found between 3D MUST-T2 and the ground-truth T2 values obtained with SE, with high coefficients of determination ($R^2 > 0.99$) for all acceleration factors (1x to 5x), suggesting high accuracy of the proposed 3D sequence even for high acceleration factors. Lower linear correlation ($R^2 = 0.95$) was observed for conventional 2D T2p-SSFP in comparison to reference SE measurements. Bias between SE and 2D T2p-SSFP with linear order acquisitions has been reported previously (3).

Bland-Altman analysis demonstrated good T2 agreement for all 31 slices of 3D MUST-T2 (Supporting Information Figure S5). The mean differences with 95% confidence interval (CI) between 3D MUST-T2 and SE were 0.6 ms (95% CI, -2.1 ms to 0.89 ms) for short T1 myocardium ([T2,T1] = [48,803] ms), 0.6 ms (95% CI, -3.7 to 2.5 ms to ms) for medium T1 myocardium ([T2,T1] = [48,1090] ms), and 1.4 ms (95% CI, -4.9 ms to -2.0 ms) for long T1 myocardium ([T2,T1] = [50,1333] ms).

In Vivo Experiments

All healthy subject and patient acquisitions/reconstructions were performed successfully, and analysis results are reported hereafter.

Healthy Subjects

For Peer Review

The average acquisition time of the proposed free-breathing 3D MUST-T2 sequence in healthy subjects was 6min43s ± 1min37s (range 4–10 minutes, heart rate range: 38–85 bpm) with 100% scan efficiency. Translational motion estimation and correction was performed in about 20s, while the average reconstruction time (including HD-PROST reconstruction and dictionary matching) was about 3 min.

Representative T2 maps from three healthy subjects acquired with the proposed 3D MUST-T2 sequence and the conventional 2D T2p-SSFP sequence are shown in Figure 4. Both free-breathing 3D MUST-T2 and breath-held 2D T2p-SSFP show ~~excellent overall visual image quality and image sharpness.~~comparable visualization of the left ventricle and surrounding structures (e.g., papillary muscles). Reconstructed T2 maps from additional healthy subjects are shown in Supporting Information Figure S6 and Supporting Information Figure S7.

Commented [BA2]: R2.1

Bull's eye plots based on the AHA's 16-segment model of the left ventricle obtained with 3D MUST-T2 and 2D T2p-SSFP mappings are depicted in Figure 5a. A small, although significant, overestimation of regional T2 values, over the whole myocardium, was observed with 3D MUST-T2 in comparison to 2D T2p-SSFP mapping (50.7 ± 1.7 ms for 3D MUST-T2 versus 48.2 ± 1.3 ms for 2D T2p-SSFP, $P < 0.05$). We found no statistical differences in regional T2 values between segments with 3D MUST-T2 for all subjects ($P = 0.6$). A small overestimation of septal T2 values was observed with 3D MUST-T2 in comparison to 2D T2p-SSFP mapping with linear k-space reordering (mean difference: -4.2 ms, ±95% confidence interval: -10.4/2.0 ms, Figure 5b). Precision of T2 values was similar for both techniques (5 ± 1 ms for 3D MUST-T2 versus 4 ± 2 ms for 2D T2p-SSFP, $P = 0.520$, Figure 5c). The corresponding average coefficient of variation for the proposed 3D MUST-T2 approach was similar to that of the 2D conventional sequence (9.13% versus 9.09%, respectively, $P = 0.097$). There were no statistical differences in mean T2 values with 3D MUST-T2 among basal, mid-ventricular and apical slices for all subjects ($P = 0.655$).

For Peer Review

The effect of heart rate differences across healthy subjects on T2 values is shown in Figure 2d. T2 measurements obtained from 3D MUST-T2 in vivo showed no significant correlation with heart rate ($T2 = 0.026 \times heart\ rate + 49$ ms, $P = 0.919$).

Eight short-axis slices of the left ventricular myocardium for one representative healthy subject obtained with the proposed 3D MUST-T2 approach are shown in Figure 6. The reconstructed T2w images and the corresponding T2 maps are included. ~~Good visual image quality (i.e. no significant artifact and minimal to no blurring) can be observed on the native T2w images for the entire left ventricle and surrounding structures (e.g. papillary muscles).~~ No noticeable residual undersampling artifacts were observed on the native T2w images, and corresponding T2 maps, for the entire left ventricle.

Commented [BA3]: R2.1

Since MUST-T2 acquisitions were performed with isotropic spatial resolution and whole-heart coverage, the T2 maps can be reformatted in any arbitrary plane. This advantage is best appreciated in Figure 7, where reformats in multiple standard orientations (short-axis, vertical long-axis, three-chamber and four-chamber) are shown for a healthy subject.

The need for using 2D iNAVs to correct for respiratory motion is shown in Supporting Information Figure S8, where the T2 maps of two healthy subjects are shown with and without 2D translational motion correction. Motion corrected T2 maps result in ~~sharper images~~better visualization of the myocardium as compared to the non-motion-corrected T2 maps, which show some spatial blurring.

Commented [BA4]: R2.1

Patients

No cardiac findings were observed in the patient study. The acquisition times of the proposed 3D MUST-T2 sequence were 7 min 23 seconds (patient #1, mean heart rate: 75 bpm) and 8 min 43 seconds (patient #2, mean heart rate: 65 bpm). Figure 8 depicts the reconstructed apical, mid-cavity and basal T2 map slices, for the two patients, using the proposed 3D MUST-T2 framework compared with the current clinical reference maps (breath-held 2D T2p-SSFP). The proposed 3D MUST-T2 produces T2 maps with visual appearance comparable to the conventional 2D T2p-SSFP technique. Mean septal T2

Commented [BA5]: R2.1

For Peer Review

relaxation times were similar between the two techniques (mid-ventricular slice: patient #1: 48.2 ± 4 ms 3D MUST-T2 versus 46.3 ± 3 ms 2D T2p-SSFP, and patient #2: 51.7 ± 7 ms 3D MUST-T2 versus 50.8 ± 4 ms 2D T2p-SSFP).

DISCUSSION

In this study, we proposed a framework for highly accelerated free-breathing whole-heart T2 mapping that combines 2D translational respiratory motion correction, with a golden angle variable density spiral-like Cartesian trajectory and a recently introduced HD-PROST reconstruction. The proposed 3D MUST-T2 approach enables accurate and precise high-resolution isotropic ($1.5mm^3$) 3D whole-heart T2 mapping acquisitions in a fast and predictable scan time.

The performance of the proposed 3D T2 mapping framework was assessed in simulations, phantom experiments, and ten healthy subjects, while initial clinical feasibility was demonstrated in two patients with suspected cardiovascular disease.

3D MUST-T2 uses a saturation pulse to reset the magnetization immediately after the R-wave, as proposed by Ding et al. (17), and thus is mostly independent of heart rate variations. Another advantage of using saturation pulses compared to other T2 mapping techniques (3,5,16,31) is that recovery periods between subsequent heartbeats are not needed, thus reducing the total acquisition time.

Further acceleration through undersampling is crucial to achieve high isotropic resolution in a clinically feasible scan time. In phantom experiments, we observed that acceleration factors of up to 5-fold led to accurate T2 values ($R^2 > 0.99$) with respect to reference SE measurements. Besides the use of an efficient undersampling trajectory, the acquisition of low-resolution 2D iNAVs at every heartbeat also permits a substantial reduction in scan time by allowing 100% respiratory scan efficiency (no data rejection) and predictable scan time (24), as opposed to other respiratory-gated T2 mapping techniques based on dNAV acquisition (17). Other free-breathing T2 mapping techniques have been proposed to allow for 100% scan efficiency and predictable scan time. Van Heeswijk et al. (5) proposed a

For Peer Review

respiratory self-navigated 3D sequence to acquire isotropic 3D T2 maps with resolution of 1.7 mm^3 in a predictable scan time of ~18min at 3T, while Basha et al. (32) proposed a 2D multi-slice sequence with slice tracking. The significant scan time reduction achieved with 3D MUST-T2 was exploited to acquire in vivo isotropic whole-heart Cartesian T2 maps in clinically feasible scan times (~8 min), while a fully sampled acquisition would have required >35 mins. The total imaging time for 3D MUST-T2 being mainly affected by the subject's heart rate and the number of slices needed to cover the whole-heart in the anterior-posterior direction. For comparison, the conventional breath-hold 2D T2p-SSFP sequence would have required between 5 and 7 minutes to cover the entire heart (assuming 7 s breathing commands, 10 s resting time between acquisitions, 10 s breath-hold, and assuming that 11 to 16 slices are needed to cover the heart). The proposed 3D T2 mapping sequence can also be performed with lower anisotropic resolution (e.g., 2.0 x 2.0 x 6.0 mm^3 as achieved in (16)), that will result in shorter scan times and inherently co-registered slices due to the 3D nature of the acquisition.

The acquisition of undersampled data comes, however, at the cost of significant loss of information which needs to be recovered. Multi-contrast HD-PROST reconstruction takes advantage of the local, non-local and contrast redundancies found in the T2w images, to recover whole-heart T2 maps with negligible remaining aliasing artifacts. The measurements of myocardial T2 values by 3D MUST-T2 in healthy subjects (average septal T2 = 50.8 ± 3 ms) were in good agreement with in vivo values published in a previous study at 1.5T with centric ordering (T2 = 50 ± 4 ms (33)). T2 overestimation with respect to the conventional breath-hold 2D T2p-SSFP sequence was observed, with a bias of 4.2 ± 6.2 ms. This overestimation was likely due to the choice of centric (3D MUST-T2) versus linear (2D T2p-SSFP) k-space ordering, as observed by Giri et al. (3). Other confounding factors such as heart rate variations (34), not present in the phantom study, or the use of fat saturation and adiabatic T2 preparation pulses could also explain this overestimation in vivo and will be further explored.

Commented [BA6]: R2.1

Although high acceleration factors were reached with the proposed 3D sequence, precision of T2 values in vivo did not show significant deviations from the conventional 2D T2p-

For Peer Review

SSFP acquisitions (4.6 ± 1 ms vs. 4.3 ± 2 ms, $P = 0.520$), and were similar to previously reported values at 3T (5,17). This can be attributed to the good performance of HD-PROST reconstruction in concert with the VD-CASPR trajectory, which limits the propagation of noise in the T2w images, noise being a severe side effect of saturation-based MR mapping techniques (16,35,36).

Dictionary-based matching was used in this study to accurately estimate myocardial T2 values by pre-generating a dictionary representative of the proposed T2 mapping sequence, and whose elements are composed of simulated signal evolution curves (28). Our findings in phantom experiments showed that dictionary-based matching has the potential to accurately estimate myocardial T2 values acquired with both 3D MUST-T2 and conventional T2p-bSSFP, whereas a T2 bias was observed with conventional mono-exponential fitting for both methods (Supporting Information Figure S4). This can be partly explained by the fact that mono-exponential fitting does not accurately describe the acquisition parameters and the signal evolution during acquisition, such as bSSFP T1/T2 ratio of tissue, subject-specific heart-rate, number of segments per heartbeat, and number of linear ramp-up pulses. Therefore, the use of dictionary-based matching could also improve conventional 2D T2p-SSFP and potentially reduce the bias observed with linear phase encoding.

Commented [BA7]: R1.1

A limitation of the current framework is that only 2D translation respiratory motion correction was performed to ensure fast reconstruction times. It has been shown in previous reports that non-rigid motion registration can improve reproducibility and spatial variability of 2D T2 mapping techniques (8,11). While this issue was not shown to be significant in the present experiments, it can be overcome by incorporating 3D non-rigid respiratory motion correction directly in the image reconstruction (37–39). Another alternative to deal with large motion between the T2w images is to extend the proposed HD-PROST reconstruction to enable motion-resolved reconstruction by extending the searching neighborhood for patch selection to the spatial-temporal dimension (40).

For Peer Review

In this study, mid-diastolic imaging was employed to minimize cardiac motion and guarantee long saturation times. However, in subjects with highly variable heart rates or high heart rates, end-systolic imaging may be preferred. Future studies will investigate the effect of shorter saturation times on the accuracy and precision of saturation-based T2 mapping, however our phantom experiments demonstrate that accuracy is not affected for different heart rates between 50 and 100 bpm.

Moreover, incomplete saturation of fat signal can occur in some regions of the T2w images, especially around the epicardial fat area. This effect can lead to fat-myocardium partial volume effect, apparent distortion and loss of sharpness on the T2 map and may alter the T2 measurements. Further optimized fat suppression for each T2w image will be investigated in the future to alleviate this difficulty.

Translational motion estimation and correction was performed inline in the scanner software while HD-PROST reconstruction and dictionary matching were performed offline. The efficient multithreaded implementation of HD-PROST allowed for fast T2 map reconstruction (in the order of 3 minutes). Further speedup, to reach sub-minute runtime, could be achieved by implementing the reconstruction on multiple GPUs and using coil compression strategies (41).

It should be noted that 3D MUST-T2 is based on a T2-prepared sequence commonly used in coronary MR angiography (42). The acceptable contrast provided by the last T2w volume (TE_{T2prep} = 55 ms, Figures 6 and 7) could also be exploited to visualize whole heart cardiac and proximal coronary artery anatomy. Thus, 3D MUST-T2 may be used for the simultaneous assessment of cardiac and coronary anatomy and myocardial T2 relaxation times in a highly simplified and efficient single free-breathing acquisition. This additional gain could potentially benefit patients with acute non-ST-segment elevation myocardial infarction where obstructive coronary artery disease and myocardial edema are often characteristic (13).

The proposed free-breathing T2 mapping framework could benefit many cardiovascular patients with severe shortness of breath and where imaging under breath-holding is often

For Peer Review

challenging. Preliminary insights into the potential of the proposed 3D MUST-T2 mapping technique in a clinical setting was provided for two patients with suspected cardiovascular disease. While no pathologies were observed in this proof-of-concept study, scanning patients often leads to new challenges (e.g., variable heart rate, irregular breathing pattern, poor compliance), resulting in degraded image quality. Higher amplitude in respiratory motion of the heart, as provided by the 2D iNAVs, was observed in patients compared to healthy controls (Supporting Information Figure S9). Mean septal T2 values measured on the two patients were comparable to that of the healthy subjects. Besides T2 relaxation times conform to the literature (Figure 8), the 3D whole-heart isotropic coverage of the proposed technique offers the opportunity to reformat the T2 maps in any desired orientation, which can be particularly useful for the comprehensive assessment of pathological tissues with complex geometry (6).

Commented [BA8]: R3.3

The proposed framework also shares similarities with the recent qBOOST-T2 approach (43) that enables co-registered bright-blood and black-blood whole-heart imaging, together with T2 quantification and coronary lumen visualization, through the use of an inversion pulse every three heartbeats. While the latest technique may be preferred whenever coronary assessment or pre-contrast black-blood images are clinically required, a thorough comparison of the two approaches in large patient cohorts will need to be studied.

Finally, the proposed fast and efficient framework holds promise for wider cardiac applications such as high-resolution motion compensated 3D T1 mapping and 3D joint T1-T2 mapping (44–49); both of which will be investigated in future works.

CONCLUSION

A novel approach was developed to enable free-breathing whole-heart 3D T2 mapping with high isotropic spatial resolution (1.5mm^3) in a clinically feasible scan time (<8 min with 100% scan efficiency and predictable scan time). The proposed 3D MUST-T2 framework achieved accurate T2 quantification in phantom, and in vivo with fast acquisition ~~and good map quality in vivo~~. 3D-MUST T2 mapping may have potential to aid the management of many cardiomyopathies in which fast and efficient free-breathing acquisitions are key to

Commented [BA9]: R2.1

For Peer Review

patient comfort, while high isotropic resolution is crucial to accurately map tissue heterogeneity. Further studies to assess the clinical utility of 3D MUST-T2 mapping in patients with myocardial inflammation are now warranted.

ACKNOWLEDGMENTS

EPG simulations were based on the algorithm described by Dr. Matthias Weigel in (19), made available on the author's website. The authors acknowledge financial support from EPSRC EP/P001009/, EP/P032311/1, EPSRC EP/P007619, Wellcome EPSRC Centre for Medical Engineering (NS/ A000049/1), and the Department of Health via the National Institute for Health Research (NIHR) comprehensive Biomedical Research Centre award to Guy's & St. Thomas' NHS Foundation Trust in partnership with King's College London and King's College Hospital NHS Foundation Trust. The views expressed are those of the authors and not necessarily those of the NHS, the NIHR, or the Department of Health.

ORCID

Aurelien Bustin https://orcid.org/0000-0002-2845-8617

Tevfik F. Ismail https://orcid.org/0000-0002-1691-7599

Claudia Prieto https://orcid.org/0000-0003-4602-2523

René M. Botnar https://orcid.org/0000-0003-2811-2509

For Peer Review

REFERENCES

1. Guo H, Au WY, Cheung JS, et al. Myocardial T2 quantitation in patients with iron overload at 3 Tesla. J. Magn. Reson. Imaging 2009;30:394–400 doi: 10.1002/jmri.21851.

2. He T, Gatehouse PD, Anderson LJ, et al. Development of a novel optimized breathhold technique for myocardial T2 measurement in thalassemia. J. Magn. Reson. Imaging 2006;24:580–5 doi: 10.1002/jmri.20681.

3. Giri S, Chung YC, Merchant A, et al. T2 quantification for improved detection of myocardial edema. J. Cardiovasc. Magn. Reson. 2009;11:1–13 doi: 10.1186/1532-429X-11-56.

4. Haberkorn SM, Spieker M, Jacoby C, Flögel U, Kelm M, Bönner F. State of the Art in Cardiovascular T2 Mapping: on the Way to a Cardiac Biomarker? Curr. Cardiovasc. Imaging Rep. 2018;11 doi: 10.1007/s12410-018-9455-3.

5. Van Heeswijk RB, Piccini D, Feliciano H, Hullin R, Schwitter J, Stuber M. Self-navigated isotropic three-dimensional cardiac T2 mapping. Magn. Reson. Med. 2015;73:1549–1554 doi: 10.1002/mrm.25258.

6. Ding H, Schar M, Zviman MM, Halperin HR, Beinart R, Herzka DA. High-resolution quantitative 3D T2 mapping allows quantification of changes in edema after myocardial infarction. J. Cardiovasc. Magn. Reson. 2013;15:345–347 doi: 10.1186/1532-429X-15-S1-P181.

7. Van Heeswijk RB, Piccini D, Tozzi P, et al. Three-dimensional self-navigated T2 mapping for the detection of acute cellular rejection after orthotopic heart transplantation. Transplant. Direct 2017;3 doi: 10.1097/TXD.0000000000000635.

8. Roujol S, Basha T, Weingartner S, et al. Motion correction for free breathing quantitative myocardial T2 mapping: impact on reproducibility and spatial variability. J. Cardiovasc. Magn. Reson. 2015;17:W5 doi: 10.1186/1532-429X-17-S1-W5.

For Peer Review

9. Jin N, Da Silveira JS, Jolly MP, et al. Free-breathing myocardial T2 mapping using GRE-EPI and automatic Non-rigid motion correction. J. Cardiovasc. Magn. Reson. 2015;17 doi: 10.1186/s12968-015-0216-z.

10. Odille F, Escanyé JM, Atkinson D, Bonnemains L, Felblinger J. Nonrigid registration improves MRI T2 quantification in heart transplant patient follow-up. J. Magn. Reson. Imaging 2015;42:168–174 doi: 10.1002/jmri.24741.

11. Giri S, Shah S, Xue H, et al. Myocardial T2 mapping with respiratory navigator and automatic nonrigid motion correction. Magn. Reson. Med. 2012;68:1570–1578 doi: 10.1002/mrm.24139.

12. Rauhalammi S, Layland J, Carrick D, et al. T1 and T2 Mapping Have Higher Diagnostic Accuracy for the Ischaemic Area-at-risk in Nstemi Patients Compared with Dark Blood Imaging. Heart 2014;100 doi: 10.3109/02699052.2014.892379.

13. Tessa C, Del Meglio J, Lilli A, et al. T1 and T2 mapping in the identification of acute myocardial injury in patients with NSTEMI. Radiol. Medica 2018;123:926–934 doi: 10.1007/s11547-018-0931-2.

14. Puntmann VO, Isted A, Hinojar R, Foote L, Carr-White G, Nagel E. T1 and T2 Mapping in Recognition of Early Cardiac Involvement in Systemic Sarcoidosis. Radiology 2017;285:63–72 doi: 10.1148/radiol.2017162732.

15. Van Heeswijk RB, Feliciano H, Bongard C, et al. Free-breathing 3T magnetic resonance T2-mapping of the heart. JACC Cardiovasc. Imaging 2012;5:1231–1239 doi: 10.1016/j.jcmg.2012.06.010.

16. Yang HJ, Sharif B, Pang J, et al. Free-breathing, motion-corrected, highly efficient whole heart T2 mapping at 3T with hybrid radial-cartesian trajectory. Magn. Reson. Med. 2016;75:126–36 doi: 10.1002/mrm.25576.

17. Ding H, Fernandez-De-Manuel L, Schär M, et al. Three-dimensional whole-heart T2 mapping at 3T. Magn. Reson. Med. 2015;74:803–816 doi: 10.1002/mrm.25458.

For Peer Review

18. Bustin A, Cruz G, Jaubert O, Lopez K, Botnar RM, Prieto C. High-dimensionality undersampled patch-based reconstruction (HD-PROST) for accelerated multi-contrast magnetic resonance imaging. Magn. Reson. Med. 2019;81:3705–3719 doi: 10.1002/mrm.27694.

19. Weigel M. Extended phase graphs: Dephasing, RF pulses, and echoes - Pure and simple. J. Magn. Reson. Imaging 2015;41:266–295 doi: 10.1002/jmri.24619.

20. Nezafat R, Stuber M, Ouwerkerk R, Gharib AM, Desai MY, Pettigrew RI. B1-insensitive T2 preparation for improved coronary magnetic resonance angiography at 3T. Magn. Reson. Med. 2006;55:858–64 doi: 10.1002/mrm.20835.

21. Prieto C, Doneva M, Usman M, et al. Highly efficient respiratory motion compensated free-breathing coronary MRA using golden-step Cartesian acquisition. J. Magn. Reson. Imaging 2015;41:738–746 doi: 10.1002/jmri.24602.

22. Bustin A, Ginami G, Cruz G, et al. Five-minute whole-heart coronary MRA with sub-millimeter isotropic resolution, 100% respiratory scan efficiency, and 3D-PROST reconstruction. Magn. Reson. Med. 2019;81:102–115 doi: 10.1002/mrm.27354.

23. Winkelmann S, Schaeffter T, Koehler T, Eggers H, Doessel O. An optimal radial profile order based on the golden ratio for time-resolved MRI. IEEE Trans. Med. Imaging 2007;26:68–76 doi: 10.1109/TMI.2006.885337.

24. Henningsson M, Koken P, Stehning C, Razavi R, Prieto C, Botnar RM. Whole-heart coronary MR angiography with 2D self-navigated image reconstruction. Magn. Reson. Med. 2012;67:437–445 doi: 10.1002/mrm.23027.

25. Ginami G, Neji R, Phinikaridou A, Whitaker J, Botnar RM, Prieto C. Simultaneous bright- and black-blood whole-heart MRI for noncontrast enhanced coronary lumen and thrombus visualization. Magn. Reson. Med. 2018;79:1460–1472 doi: 10.1002/mrm.26815.

26. Bustin A, Voilliot D, Menini A, et al. Isotropic Reconstruction of MR Images Using

For Peer Review

3D Patch-Based Self-Similarity Learning. IEEE Trans. Med. Imaging 2018;37:1932–1942 doi: 10.1109/TMI.2018.2807451.

27. Hennig J, Weigel M, Scheffler K. Calculation of flip angles for echo trains with predefined amplitudes with the extended phase graph (EPG)-algorithm: principles and applications to hyperecho and TRAPS sequences. Magn. Reson. Med. 2004;51:68–80 doi: 10.1002/mrm.10658.

28. Roccia E, Vidya Shankar R, Neji R, et al. Accelerated 3D T2 mapping with dictionary-based matching for prostate imaging. Magn. Reson. Med. 2019;81:1795–1805 doi: 10.1002/mrm.27540.

29. Captur G, Gatehouse P, Keenan KE, et al. A medical device-grade T1 and ECV phantom for global T1 mapping quality assurance - the T1 Mapping and ECV Standardization in cardiovascular magnetic resonance (T1MES) program. J. Cardiovasc. Magn. Reson. 2016;18:1–20 doi: 10.1186/s12968-016-0280-z.

30. Cerqueira MD, Weissman NJ, Dilsizian V, et al. Standardized myocardial segmentation and nomenclature for tomographic imaging of the heart: a statement for healthcare professionals from the cardiac imaging. Circulation 2002;105 doi: 10.1161/hc0402.102975.

31. Darçot E, Yerly J, Colotti R, et al. Accelerated and high-resolution cardiac T2 mapping through peripheral k-space sharing. Magn. Reson. Med. 2019;81:220–233 doi: 10.1002/mrm.27374.

32. Basha TA, Bellm S, Roujol S, Kato S, Nezafat R. Free-breathing slice-interleaved myocardial T2 mapping with slice-selective T2 magnetization preparation. Magn. Reson. Med. 2016;76:555–565 doi: 10.1002/mrm.25907.

33. Blume U, Lockie T, Stehning C, et al. Interleaved T1 and T2 relaxation time mapping for cardiac applications. J. Magn. Reson. Imaging 2009;29:480–487 doi: 10.1002/jmri.21652.

For Peer Review

34. Granitz M, Motloch LJ, Granitz C, et al. Comparison of native myocardial T1 and T2 mapping at 1.5T and 3T in healthy volunteers: Reference values and clinical implications. Wien. Klin. Wochenschr. 2019;131:143–155 doi: 10.1007/s00508-018-1411-3.

35. Nordio G, Bustin A, Henningsson M, et al. 3D SASHA myocardial T1 mapping with high accuracy and improved precision. Magn. Reson. Mater. Physics, Biol. Med. 2018 doi: 10.1007/s10334-018-0703-y.

36. Bustin A, Ferry P, Codreanu A, et al. Impact of denoising on precision and accuracy of saturation-recovery-based myocardial T1 mapping. J. Magn. Reson. Imaging 2017;46:1377–1388 doi: 10.1002/jmri.25684.

37. Odille F, Menini A, Escanye J-M, et al. Joint reconstruction of multiple images and motion in MRI: application to free-breathing myocardial T2 quantification. IEEE Trans. Med. Imaging 2016;35:197–207 doi: 10.1109/TMI.2015.2463088.

38. Batchelor PG, Atkinson D, Irarrazaval P, Hill DLG, Hajnal J, Larkman D. Matrix description of general motion correction applied to multishot images. Magn. Reson. Med. 2005;54:1273–1280 doi: 10.1002/mrm.20656.

39. Cruz G, Atkinson D, Henningsson M, Botnar RM, Prieto C. Highly efficient nonrigid motion-corrected 3D whole-heart coronary vessel wall imaging. Magn. Reson. Med. 2017;77:1894–1908 doi: 10.1002/mrm.26274.

40. Kuestner T, Bustin A, Cruz G, et al. 3D Cartesian free-running cardiac and respiratory resolved whole-heart MRI. In: Proceedings of the 27th Annual Meeting of ISMRM Montreal Canada. ; 2019. p. 2192.

41. Zhang T, Pauly JM, Vasanawala SS, Lustig M. Coil compression for accelerated imaging with Cartesian sampling. Magn. Reson. Med. 2013;69:571–82 doi: 10.1002/mrm.24267.

42. Botnar RM, Stuber M, Danias PG, Kissinger K V, Manning WJ. Improved coronary

For Peer Review

artery definition with T2-weighted, free-breathing, three-dimensional coronary MRA. Circulation 1999;99:3139–3148 doi: 10.1161/01.CIR.99.24.3139.

43. Milotta G, Ginami G, Bustin A, Neji R, Prieto C, Botnar RM. 3D whole-heart free-breathing BOOST-T2 mapping. In: Proceedings of the 27th Annual Meeting of ISMRM Montreal Canada. ; 2019. p. 2002.

44. Akçakaya M, Weingärtner S, Basha TA, Roujol S, Bellm S, Nezafat R. Joint myocardial T1 and T2 mapping using a combination of saturation recovery and T2-preparation. Magn. Reson. Med. 2016;76:888–896 doi: 10.1002/mrm.25975.

45. Kvernby S, Warntjes MJ an B, Haraldsson H, Carlhäll CJ, Engvall J, Ebbers T. Simultaneous three-dimensional myocardial T1 and T2 mapping in one breath hold with 3D-QALAS. J. Cardiovasc. Magn. Reson. 2014;16:102 doi: 10.1186/s12968-014-0102-0.

46. Xanthis CG, Bidhult S, Greiser A, et al. Simulation-based quantification of native T1 and T2 of the myocardium using a modified MOLLI scheme and the importance of Magnetization Transfer. Magn. Reson. Imaging 2018;48:96–106 doi: 10.1016/j.mri.2017.12.020.

47. Guo R, Chen Z, Herzka DA, Luo J, Ding H. A three-dimensional free-breathing sequence for simultaneous myocardial T1 and T2 mapping. Magn. Reson. Med. 2018:1031–1043 doi: 10.1002/mrm.27466.

48. Santini F, Kawel-Boehm N, Greiser A, Bremerich J, Bieri O. Simultaneous T1 and T2 quantification of the myocardium using cardiac balanced-SSFP inversion recovery with interleaved sampling acquisition (CABIRIA). Magn. Reson. Med. 2015;74:365–371 doi: 10.1002/mrm.25402.

49. Milotta G, Ginami G, Bustin A, Neji R, Prieto C, Botnar RM. 3D Whole-heart High-resolution Motion Compensated Joint T1/T2 Mapping. In: Proceedings of the 27th Annual Meeting of ISMRM Montreal Canada. ; 2019. p. 2003.

For Peer Review

Figure Captions

Figure 1 Schematic overview of the proposed free-breathing 3D MUST-T2 technique for whole-heart myocardial T2 mapping. Three T2-prepared volumes are acquired sequentially with increasing TE_{T2prep} ([0,28,55] ms). A nonselective saturation pulse is applied immediately after the ECG R-wave to avoid recovery heartbeats. A 2D image-navigator is acquired to enable translational respiratory motion correction of the heart and shorter and predictable scan times. A golden-angle shifted variable density Cartesian undersampling is employed to achieve clinically feasible scan times. All T2 prepared volumes are reconstructed simultaneously with HD-PROST (18). A dictionary is then simulated and matched to the measured signal to generate the whole-heart T2 maps. Abbreviations: TD, trigger delay; T_{SAT}, saturation time; AW, acquisition window

Figure 2 Results from EPG simulations show the effect of the saturation pulse on the MR signal evolution. (A) shows the simulated magnetization obtained with the EPG formalism for different recovery times (ranging from 0 to 9 seconds) when the saturation pulse is not used. The signals were generated for tissues with a T2 of 50 ms, varying T1s (ranging from 700 ms to 1200 ms), TE_{T2prep} = 50 ms, and a simulated heart rate of 60 bpm. For long T1s, a minimum of ~6 idle heartbeats are needed to allow for full recovery of the longitudinal magnetization. When the saturation pulse is applied at every heartbeat (B), idle heartbeats are not required for signal recovery, at the cost of lower signal intensity. (C) Evolution of the matched T2 values obtained with the proposed 3D MUST-T2 mapping sequence over different simulated heart rates (ranging from 50 bpm to 100 bpm) for each phantom vial. The proposed approach is mostly insensitive to heart rate variations, even for long T1s. (D) The effect of different heart rates across all healthy subjects (N = 10) on mean T2 values is shown.

Figure 3 Phantom accuracy for the proposed 3D MUST-T2 sequence. Plots are comparing the mean T2 values derived from the nine vials for five different acceleration factors with the ground truth T2 values (measured by SE with eight TEs from 10-640 ms (29)), conventional 2D T2p-SSFP mapping (green) and the proposed 3D MUST-T2 sequence. T2

For Peer Review

accuracy is preserved with the proposed approach with excellent agreement with the reference T2 values, even for high acceleration (x5). T2 values for the last tube (T2 = 250ms) were out of range (>300 ms) for the 2D T2p-SSFP sequence and therefore are not shown.

Figure 4 T2 maps obtained using the proposed free-breathing 3D MUST-T2 sequence and the conventional breath-held 2D T2p-SSFP sequence are shown for three healthy subjects. 3D MUST-T2 slices were reformatted to short-axis to match the 2D T2 map acquisitions. ~~High visual image quality and sharpness can be observed on the 3D MUST-T2 maps with clear delineation~~Good visualization of the myocardium and surrounding structures can be observed on the 3D MUST-T2 maps. Acquisition times are expressed as [min:sec]. Abbreviations: BPM, beats per minute; AT, acquisition time

Commented [BA10]: R2.1

Figure 5 Accuracy and precision of the proposed 3D MUST-T2 mapping sequence. (A) T2 accuracy of the proposed 3D MUST-T2 sequence versus conventional 2D T2p-SSFP, as measured by the mean T2 value are shown in the left ventricular segmentation. T2 values are in good agreement with the literature (T2 = 50 ± 4 ms (33)). The averaged T2 relaxation times over the whole myocardium are shown in the bull's eye plots' center. Accuracy (B) and precision (C) of T2 relaxation times (ms) obtained in the myocardial septum with the proposed 3D MUST-T2 and the conventional 2D T2p-SSFP are shown for the 10 healthy subjects.

Figure 6 Three-dimensional visualization of the acquired T2w images and the corresponding T2 volume. Representative T2w images for subject 2 (acquisition time: 10 min, heart rate = 38 bpm), and the corresponding T2 maps obtained by the proposed 3D MUST-T2. Eight reformatted short-axis slices that cover the heart from apex to base are shown. Uniform distribution of T2 values through the slices over the whole-left ventricle can be observed. The color scale indicates T2 values between 0-120 ms.

Figure 7 Representative T2-prepared images for subject 2 and the corresponding T2 maps obtained with the proposed 3D MUST-T2 sequence. Reformats in short-axis, vertical long-axis, 3-chamber and 4-chamber views are shown.

For Peer Review

Figure 8 Short-axis T2 maps at apical, mid-ventricular and basal level for two patients acquired with the proposed free-breathing 3D MUST-T2 framework and the conventional breath-hold 2D T2p-SSFP sequence. The septal T2 relaxation times for each slice are reported as mean ± standard deviation.

Supporting Information Figure Captions

Additional Supporting Information may be found in the online version of this article.

Supporting Information Figure S1 A 3D Cartesian variable-density trajectory was employed to allow for fast acquisition of multiple T2w images. The Cartesian trajectory with spiral order samples the k_y-k_z phase encoding plane following approximate spiral interleaves on the Cartesian grid with variable density along each spiral arm. In this sketch, the 2 first acquired spirals are shown for each contrast, each spiral containing 20 segments. A golden angle rotation between successive spirals and successive contrasts is applied to introduce incoherently distributed aliasing artifacts along the contrast dimension, and noise-like artifacts in the spatial dimension.

Supporting Information Figure S2 Flowchart of the optimization 2 of the proposed High-Dimensionality Patch-based RecOnSTruction (HD-PROST). Denoising of multiple T2w images is performed using a 3D block matching, which groups and unfolds similar 3D patches in the noisy multi-contrast images to form a low-rank 2D matrix. A third-order tensor is formed by stacking the T2 contrast dimension on the third dimension. The high-order tensor of size N (number of pixels in each patch) x K (number of similar patches within a neighborhood) x L (number of T2 contrasts) admits a low multilinear rank approximation and can be compressed, through high-order tensor decomposition, by truncating the multilinear singular vectors that correspond to small multilinear singular values. The outputs of this step are the denoised multi-contrast images which are then used in the joint regularized reconstruction step (optimization 1) as prior knowledge. Reconstruction parameters used in this study are shown (bottom row). We refer the reader to (18) for more information on these parameters. Reconstruction parameter details: N,

For Peer Review

patch size (in pixels); L, number of contrasts; K, number of similar patches; λ_p, threshold value.

Supporting Information Figure S3 Simulations of the proposed T2 mapping sequence were performed using the EPG formalism to assess the effect of T1 in the EPG-based dictionary on the matched T2 value. Signals evolutions for different T1 (from 850 to 1200 with a step size of 50 ms) and T2 (from 42 to 82 with a step size of 8 ms) were generated and matched to a dictionary simulated with fixed T1 (1100 ms) and varying T2s (similar to the one used in the phantom experiment). (A) Matched T2 is plotted as a function of T1. (B) The signal evolutions corresponding to short (T1/T2 = 800/52 ms), medium (T1/T2 = 1100/52 ms), and long (T1/T2 = 1300/52 ms) T1 myocardium were generated for the proposed sequence through EPG simulation. The obtained signal evolutions did not seem to differ, suggesting that the proposed 3D MUST-T2 map sequence with dictionary-based matching is independent of the T1 used in the EPG-based dictionary (matched T2s were the same for the three generated signals and equal to 52 ms). Therefore, for the phantom and in vivo experiments, we kept the T1 constant at 1100 ms.

Supporting Information Figure S4 Conventional mono-exponential fitting and dictionary-based matching for 2D T2p-SSFP T2 mapping in comparison to the proposed 3D MUST-T2 sequence for the phantom study. The proposed 3D acquisition with mono-exponential fitting is also included for comparison purposes. Accurate phantom T2 values, in agreement with reference spin echo, were obtained with the proposed 3D MUST-T2 sequence with dictionary-based matching, however bias is observed with the proposed acquisition when mono-exponential fitting is employed. Bias is also observed with the conventional (linear phase encoding) 2D T2p-SSFP mapping with mono-exponential fitting, however this bias is significantly reduced when dictionary-based matching is employed.

Supporting Information Figure S5 Spatial T2 uniformity over the slice direction is assessed for the phantom study for three vials (corresponding to short, medium and long T1 myocardium). The solid line is the average difference between gold-standard spin echo

For Peer Review

and the proposed 3D MUST-T2 mapping sequence, and the dashed lines represent the mean ± two standard deviations between the two techniques. Good T2 uniformity can be observed with the proposed technique. The mean difference in T2 for the vial corresponding to short T1 myocardium was -0.6 ms [±95% confidence interval (CI) = -2.1/0.89 ms), -0.6 ms [±95% CI = -3.7/2.5 ms) for the medium T1 myocardium, and -1.4 ms [±95% CI = -4.9/2.0 ms) for the long T1 myocardium.

Supporting Information Figure S6 T2 maps obtained using the proposed free-breathing 3D MUST-T2 mapping sequence and the conventional breath-held 2D T2p-SSFP sequence are shown for three additional healthy subjects. 3D MUST-T2 slices were reformatted to short-axis to match the 2D T2 map acquisitions. Representative 16 AHA segments are shown to illustrate how much spatial information was considered for T2 calculation. Acquisition times are expressed as [min:sec]. Abbreviations: BPM, beats per minute; AT, acquisition time.

Supporting Information Figure S7 Axial view of T2 maps acquired using the proposed 3D T2 mapping sequence on 3 healthy subjects. Number of slices was adjusted per subject to cover the left ventricle in the anterior-posterior direction.

Supporting Information Figure S8 Impact of iNAV-based beat-to-beat translation motion correction on 3D MUST-T2 map is shown for two healthy subjects. Reconstructed T2w images (TE_{T2prep} = 55 ms) are shown before and after motion correction with the corresponding T2 maps (A). ~~Increased image sharpness~~Better visualization of the myocardium can be observed after motion correction with clear delineation of cardiac structures and myocardial walls. Note the blurring observed on the non-motion corrected T2 maps. Plots showing the intensity profiles, taken on the T2w images through the heart-liver interface, are shown in (B). ~~Increase sharpness can be observed when translational respiratory motion correction is applied (indicated by the green lines).~~

Supporting Information Figure S9 (A) Foot-head respiratory displacements of the heart obtained from the 2D image navigators at each heartbeat are shown for 2 representative healthy subjects (left) and 2 patients (right). The end-expiration position is used as reference

Commented [BA11]: R2.1

For Peer Review

for translational motion estimation. While regular breathing patterns can be observed on the healthy subjects, more irregular breathing patterns with strong motion amplitudes are observed on patient 1 and patient 2. (B) Average R-R intervals are shown for each healthy subject and patient. Patient 1 presented with irregular cardiac rhythm (R-R = 838±211 ms).

Commented [BA12]: R3.3

For Peer Review

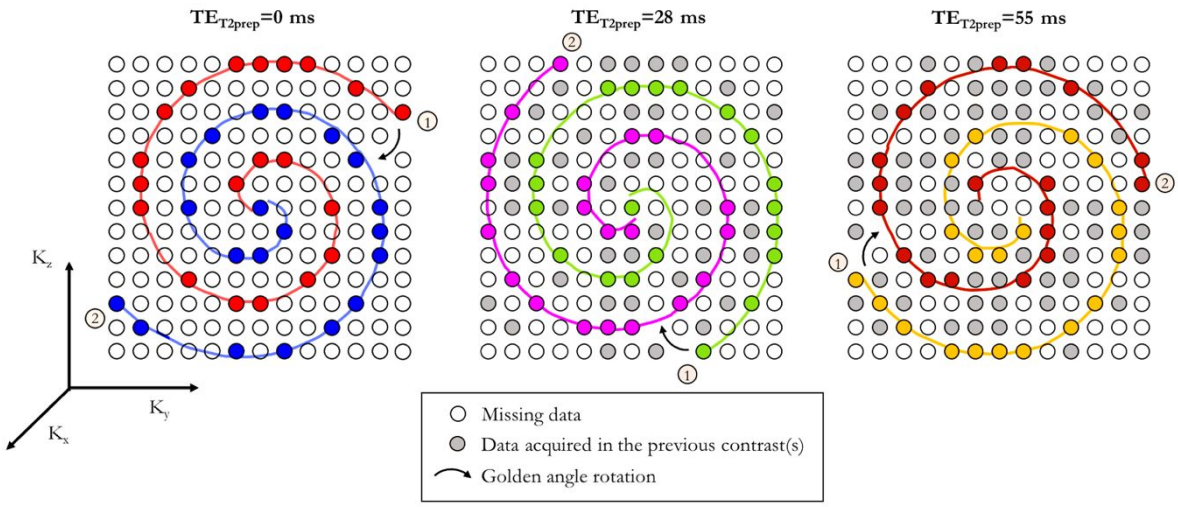

Supporting Information Figure S1 A 3D Cartesian variable-density trajectory was employed to allow for fast acquisition of multiple T2w images. The Cartesian trajectory with spiral order samples the k_y-k_z phase encoding plane following approximate spiral interleaves on the Cartesian grid with variable density along each spiral arm. In this sketch, the 2 first acquired spirals are shown for each contrast, each spiral containing 20 segments. A golden angle rotation between successive spirals and successive contrasts is applied to introduce incoherently distributed aliasing artifacts along the contrast dimension, and noise-like artifacts in the spatial dimension.

For Peer Review

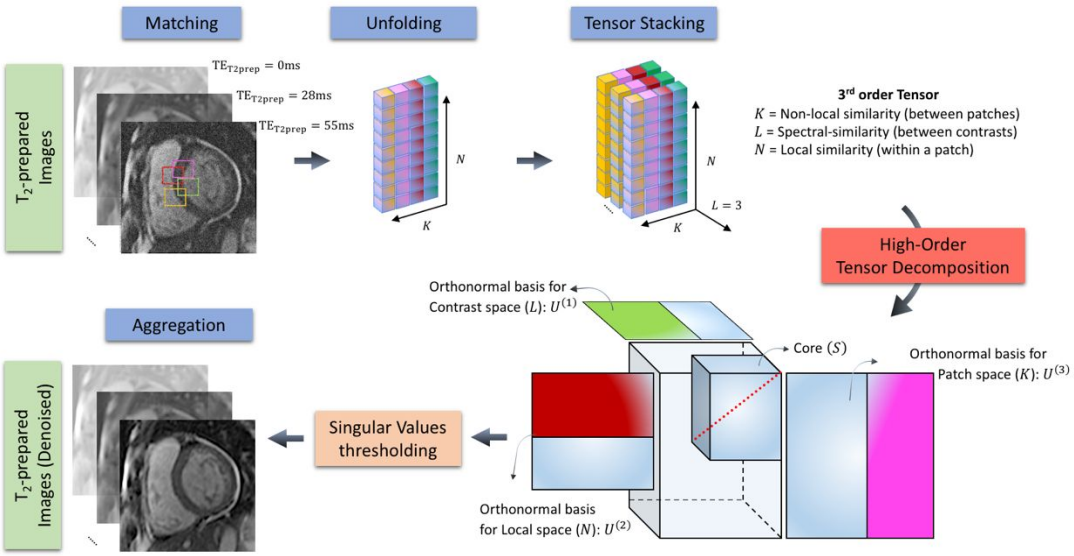

Parameters

CG iter	#Patches	λ_p	Patch size	ADMM iter	Window Search	Patch Offset
10	K=20	0.1	N=5^3	5	20	4

Supporting Information Figure S2 Flowchart of the optimization 2 of the proposed High-Dimensionality Patch-based RecOnSTruction (HD-PROST). Denoising of multiple T2w images is performed using a 3D block matching, which groups and unfolds similar 3D patches in the noisy multi-contrast images to form a low-rank 2D matrix. A third-order tensor is formed by stacking the T2 contrast dimension on the third dimension. The high-order tensor of size N (number of pixels in each patch) x K (number of similar patches within a neighborhood) x L (number of T2 contrasts) admits a low multilinear rank approximation and can be compressed, through high-order tensor decomposition, by truncating the multilinear singular vectors that correspond to small multilinear singular values. The outputs of this step are the denoised multi-contrast images which are then used in the joint regularized reconstruction step (optimization 1) as prior knowledge. Reconstruction parameters used in this study are shown (bottom row). We refer the reader to (18) for more information on these parameters. Reconstruction parameter details: N, patch size (in pixels); L, number of contrasts; K, number of similar patches; λ_p, threshold value.

For Review

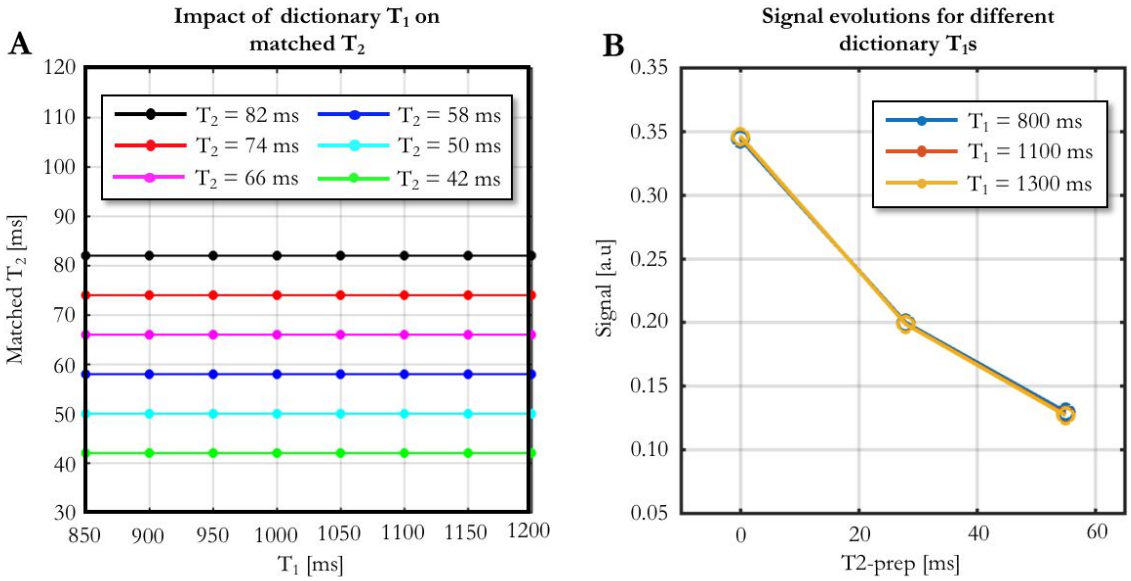

Supporting Information Figure S3 Simulations of the proposed T2 mapping sequence were performed using the EPG formalism to assess the effect of T1 in the EPG-based dictionary on the matched T2 value. Signals evolutions for different T1 (from 850 to 1200 with a step size of 50 ms) and T2 (from 42 to 82 with a step size of 8 ms) were generated and matched to a dictionary simulated with fixed T1 (1100 ms) and varying T2s (similar to the one used in the phantom experiment). (A) Matched T2 is plotted as a function of T1. (B) The signal evolutions corresponding to short (T1/T2 = 800/52 ms), medium (T1/T2 = 1100/52 ms), and long (T1/T2 = 1300/52 ms) T1 myocardium were generated for the proposed sequence through EPG simulation. The obtained signal evolutions did not seem to differ, suggesting that the proposed 3D MUST-T2 map sequence with dictionary-based matching is independent of the T1 used in the EPG-based dictionary (matched T2s were the same for the three generated signals and equal to 52 ms). Therefore, for the phantom and in vivo experiments, we kept the T1 constant at 1100 ms.

For Peer Review

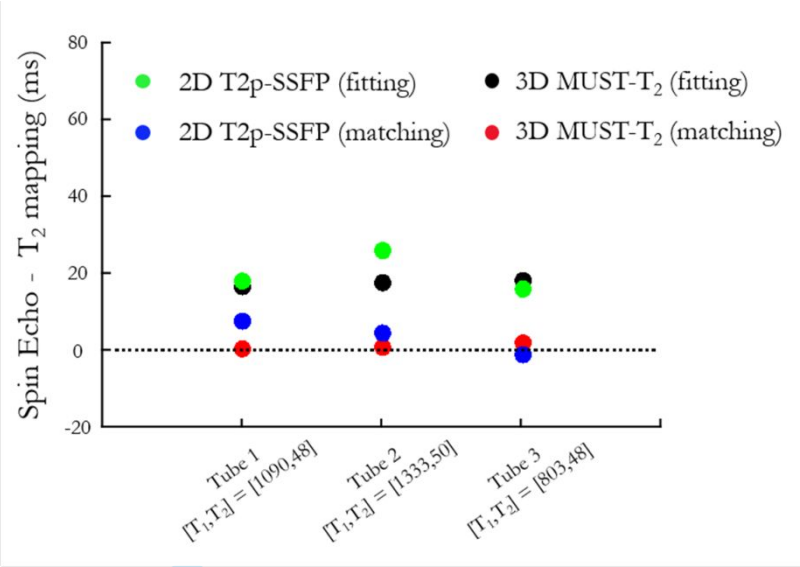

Supporting Information Figure S4 Conventional mono-exponential fitting and dictionary-based matching for 2D T2p-SSFP T2 mapping in comparison to the proposed 3D MUST-T2 sequence for the phantom study. The proposed 3D acquisition with mono-exponential fitting is also included for comparison purposes. Accurate phantom T2 values, in agreement with reference spin echo, were obtained with the proposed 3D MUST-T2 sequence with dictionary-based matching, however bias is observed with the proposed acquisition when mono-exponential fitting is employed. Bias is also observed with the conventional (linear phase encoding) 2D T2p-SSFP mapping with mono-exponential fitting, however this bias is significantly reduced when dictionary-based matching is employed.

For Peer Review

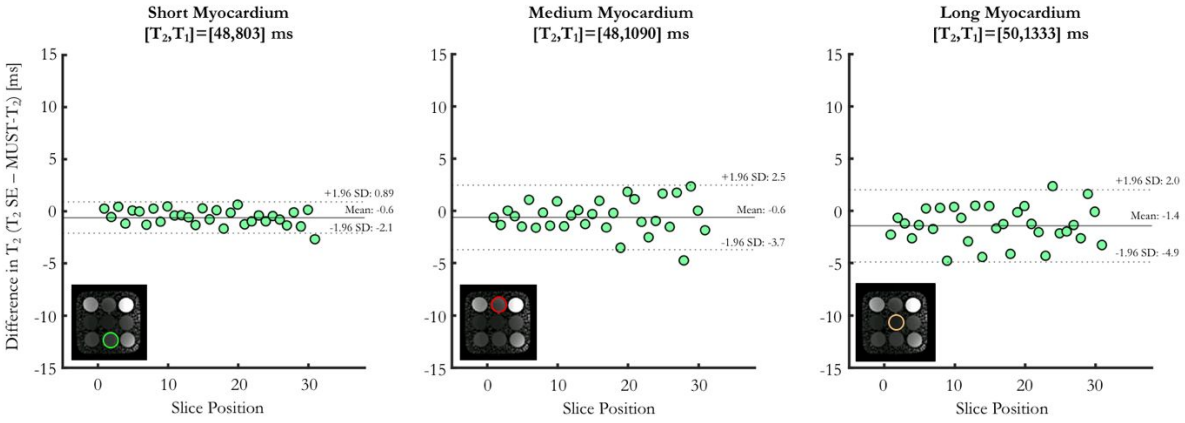

Supporting Information Figure S5 Spatial T2 uniformity over the slice direction is assessed for the phantom study for three vials (corresponding to short, medium and long T1 myocardium). The solid line is the average difference between gold-standard spin echo and the proposed 3D MUST-T2 mapping sequence, and the dashed lines represent the mean ± two standard deviations between the two techniques. Good T2 uniformity can be observed with the proposed technique. The mean difference in T2 for the vial corresponding to short T1 myocardium was -0.6 ms [±95% confidence interval (CI) = -2.1/0.89 ms), -0.6 ms [±95% CI = -3.7/2.5 ms) for the medium T1 myocardium, and -1.4 ms [±95% CI = -4.9/2.0 ms) for the long T1 myocardium.

For Peer Review

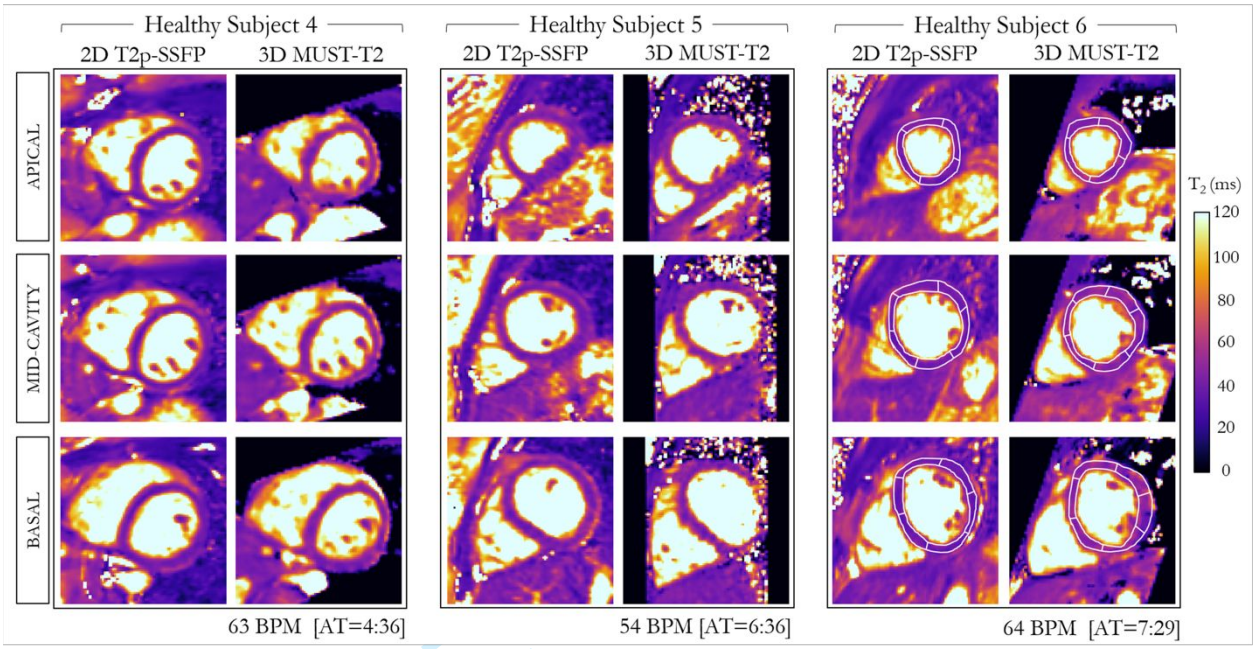

Supporting Information Figure S6 T2 maps obtained using the proposed free-breathing 3D MUST-T2 mapping sequence and the conventional breath-held 2D T2p-SSFP sequence are shown for three additional healthy subjects. 3D MUST-T2 slices were reformatted to short-axis to match the 2D T2 map acquisitions. Representative 16 AHA segments are shown to illustrate how much spatial information was considered for T2 calculation. Acquisition times are expressed as [min:sec]. Abbreviations: BPM, beats per minute; AT, acquisition time.

For Peer Review

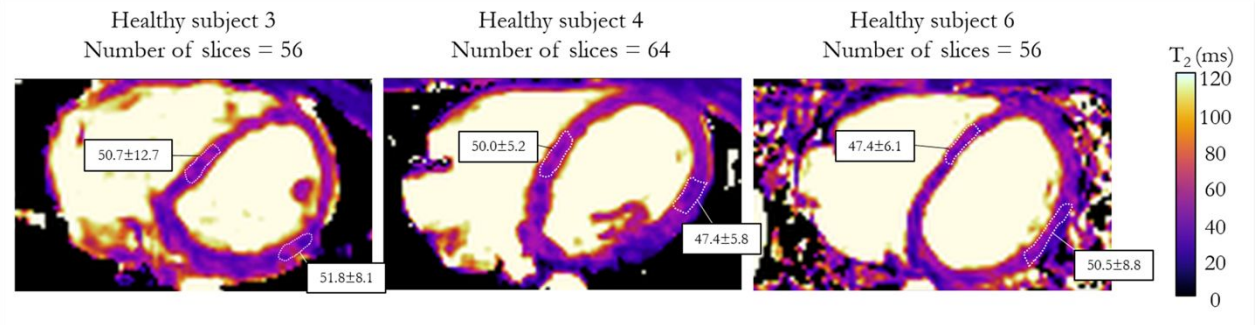

Supporting Information Figure S7 Axial view of T2 maps acquired using the proposed 3D T2 mapping sequence on 3 healthy subjects. Number of slices was adjusted per subject to cover the left ventricle in the anterior-posterior direction.

For Peer Review

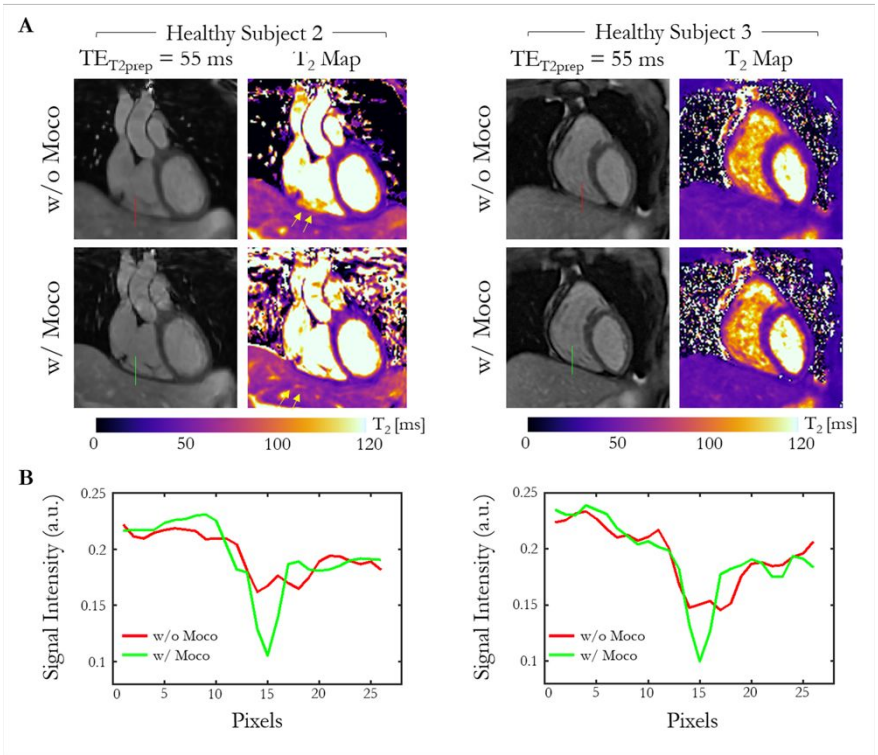

Supporting Information Figure S8 Impact of iNAV-based beat-to-beat translation motion correction on 3D MUST-T2 map is shown for two healthy subjects. Reconstructed T2w images (TE_{T2prep} = 55 ms) are shown before and after motion correction with the corresponding T2 maps (A). Better visualization of the myocardium can be observed after motion correction with clear delineation of cardiac structures and myocardial walls. Note the blurring observed on the non-motion corrected T2 maps. Plots showing the intensity profiles, taken on the T2w images through the heart-liver interface, are shown in (B).

Peer Review

A

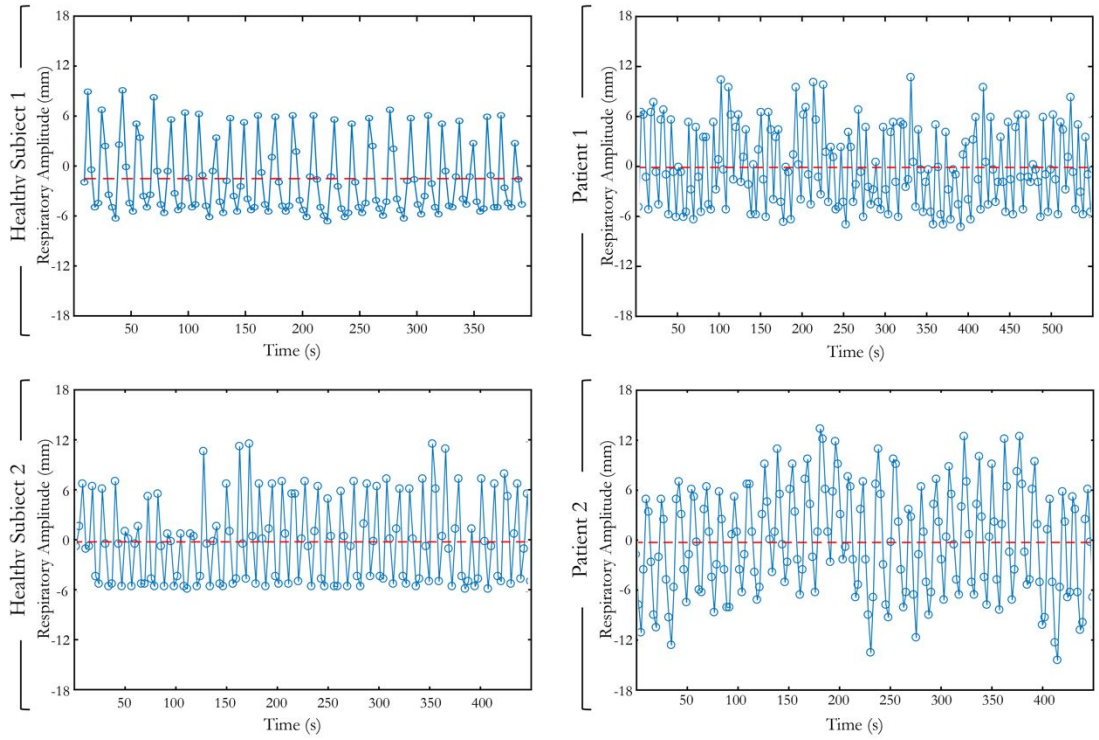

B

Subject	Subject 1	Subject 2	Subject 3	Subject 4	Subject 5	Subject 6	Subject 7	Subject 8	Subject 9	Subject 10	Patient 1	Patient 2
Average R-R interval (ms)	1118±34	1582±93	1037±37	954±36	1187±65	946±41	1021±121	741±149	1764±33	957±58	838±211	971±24

Supporting Information Figure S9 (A) Foot-head respiratory displacements of the heart obtained from the 2D image navigators at each heartbeat are shown for 2 representative healthy subjects (left) and 2 patients (right). The end-expiration position is used as reference for translational motion estimation. While regular breathing patterns can be observed on the healthy subjects, more irregular breathing patterns with strong motion amplitudes are observed on patient 1 and patient 2. (B) Average R-R intervals are shown for each healthy subject and patient. Patient 1 presented with irregular cardiac rhythm (R-R = 838±211 ms).

For Review

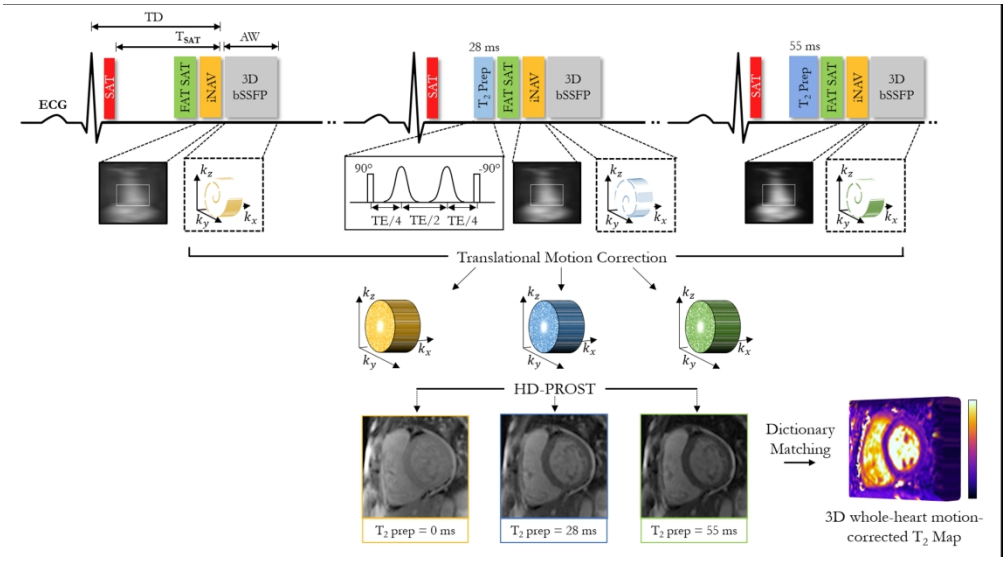

Figure 1. Schematic overview of the proposed free-breathing 3D MUST-T2 technique for whole-heart myocardial T2 mapping. Three T2-prepared volumes are acquired sequentially with increasing TE_{T2prep} ([0,28,55] ms). A nonselective saturation pulse is applied immediately after the ECG R-wave to avoid recovery heartbeats. A 2D image-navigator is acquired to enable translational respiratory motion correction of the heart and shorter and predictable scan times. A golden-angle shifted variable density Cartesian undersampling is employed to achieve clinically feasible scan times. All T2 prepared volumes are reconstructed simultaneously with HD-PROST (18). A dictionary is then simulated and matched to the measured signal to generate the whole-heart T2 maps. Abbreviations: TD, trigger delay; T_{SAT}, saturation time; AW, acquisition window.

316x175mm (300 x 300 DPI)

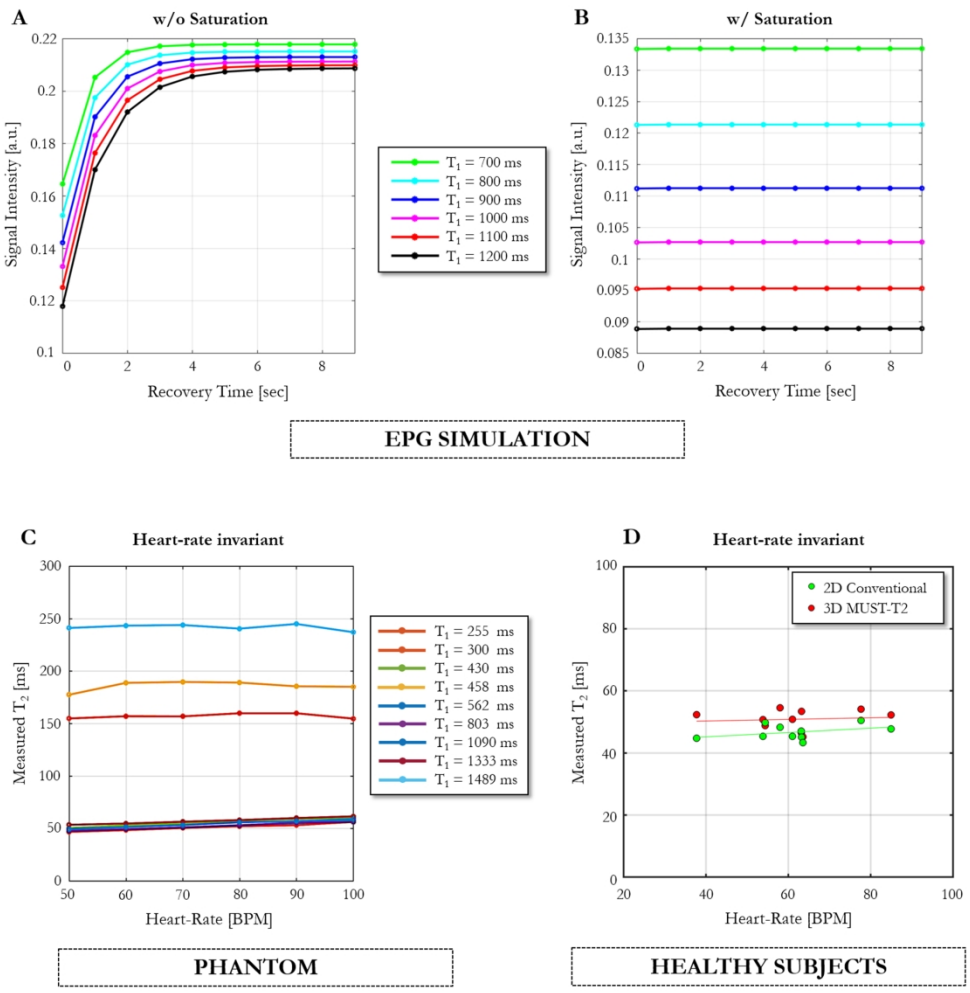

Figure 2. Results from EPG simulations show the effect of the saturation pulse on the MR signal evolution. (A) shows the simulated magnetization obtained with the EPG formalism for different recovery times (ranging from 0 to 9 seconds) when the saturation pulse is not used. The signals were generated for tissues with a T2 of 50 ms, varying T1s (ranging from 700 ms to 1200 ms), TE_{T2prep} = 50 ms, and a simulated heart-rate of 60 bpm. For long T1s, a minimum of ~6 idle heartbeats are needed to allow for full recovery of the longitudinal magnetization. When the saturation pulse is applied at every heart-beat (B), idle heartbeats are not required for signal recovery, at the cost of lower signal intensity. (C) Evolution of the matched T2 values obtained with the proposed 3D MUST-T2 mapping sequence over different simulated heart-rates (ranging from 50 bpm to 100 bpm) for each phantom vial. The proposed approach is mostly insensitive to heart-rate variations, even for long T1s. (D) The effect of different heart-rates across all healthy subjects (N = 10) on mean T2 values is shown.

274x277mm (300 x 300 DPI)

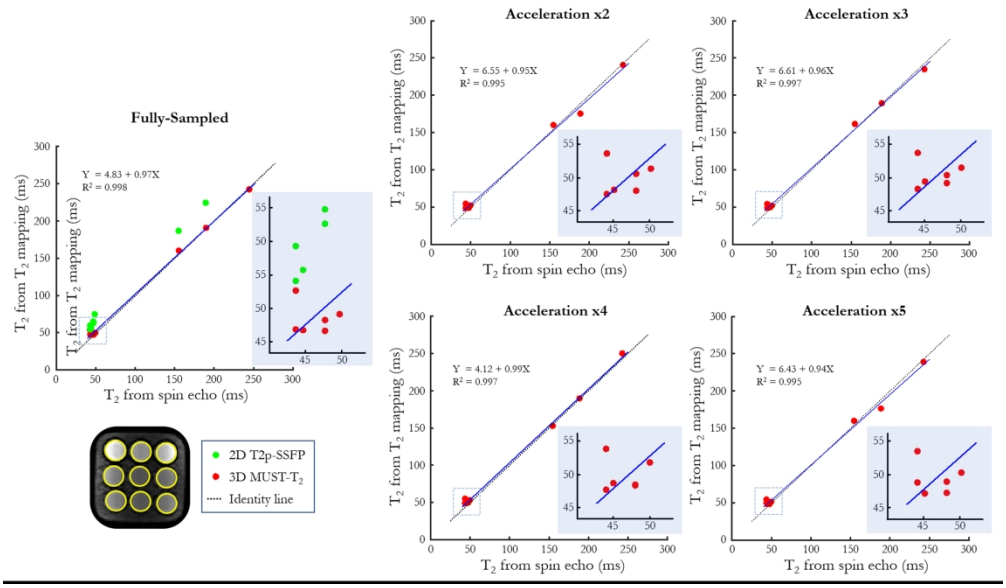

Figure 3. Phantom accuracy for the proposed 3D MUST-T2 sequence. Plots are comparing the mean T2 values derived from the nine vials for five different acceleration factors with the ground truth T2 values (measured by SE with eight TEs from 10-640 ms [29]), conventional 2D T2p-SSFP mapping (green) and the proposed 3D MUST-T2 sequence. T2 accuracy is preserved with the proposed approach with excellent agreement with the reference T2 values, even for high acceleration (x5). T2 values for the last tube (T2 = 250ms) were out of range (>300 ms) for the 2D T2p-SSFP sequence and therefore are not shown.

331x196mm (300 x 300 DPI)

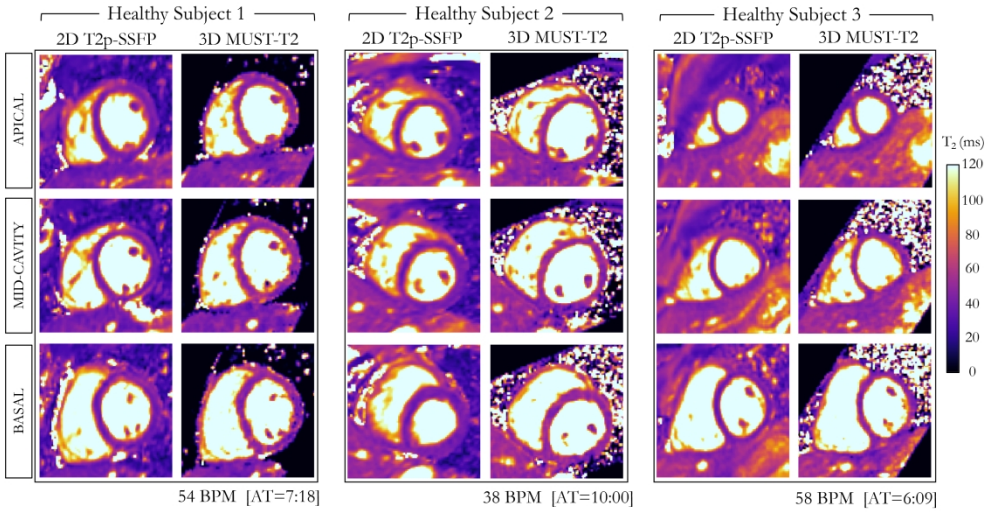

Figure 4. T2 maps obtained using the proposed free-breathing 3D MUST-T2 sequence and the conventional breath-held 2D T2p-SSFP sequence are shown for three healthy subjects. 3D MUST-T2 slices were reformatted to short-axis to match the 2D T2 map acquisitions. Good visualization of the myocardium and surrounding structures can be observed on the 3D MUST-T2 maps. Acquisition times are expressed as [min:sec]. Abbreviations: BPM, beats per minute; AT, acquisition time.

348x182mm (300 x 300 DPI)

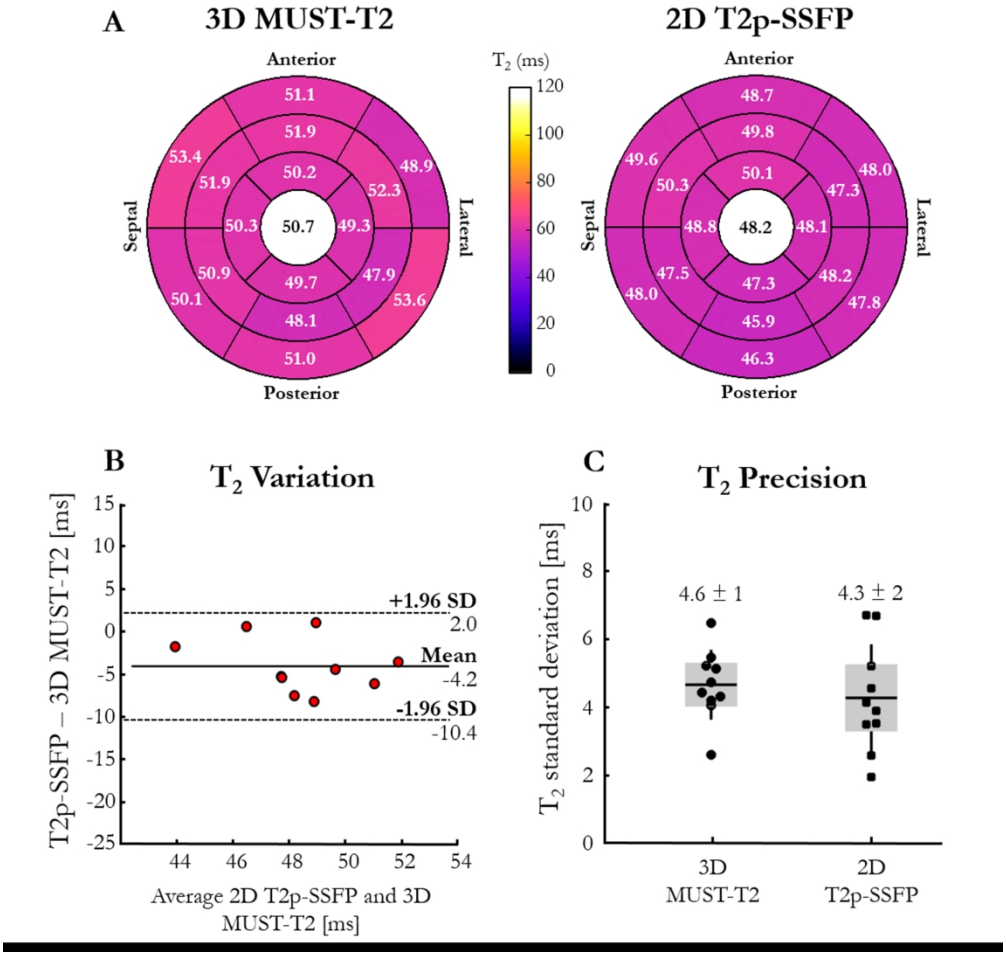

Figure 5. Accuracy and precision of the proposed 3D MUST-T2 mapping sequence. (A) T2 accuracy of the proposed 3D MUST-T2 sequence versus conventional 2D T2p-SSFP, as measured by the mean T2 value are shown in the left ventricular segmentation. T2 values are in good agreement with the literature (T2 = 50 ± 4 ms (33)). The averaged T2 relaxation times over the whole myocardium are shown in the bull's eye plots' center. Accuracy (B) and precision (C) of T2 relaxation times (ms) obtained in the myocardial septum with the proposed 3D MUST-T2 and the conventional 2D T2p-SSFP are shown for the 10 healthy subjects.

196x190mm (300 x 300 DPI)

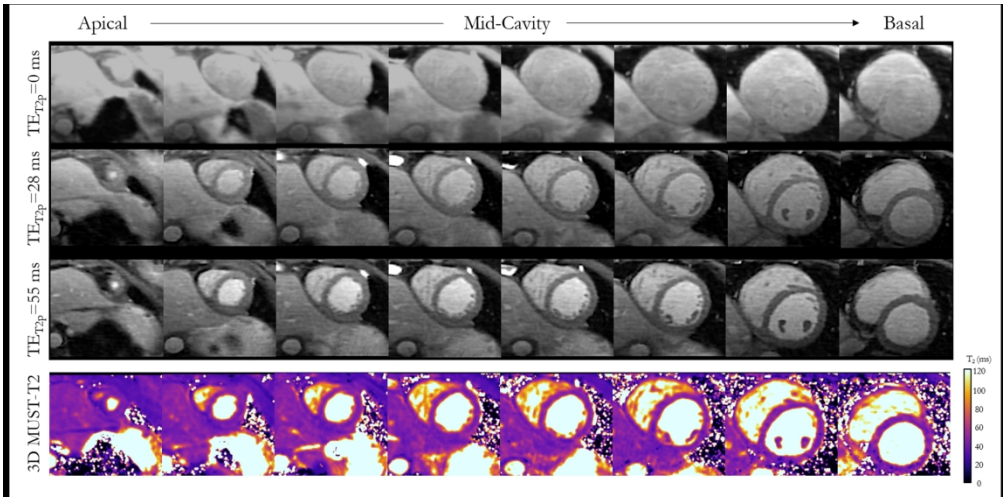

Figure 6. Three-dimensional visualization of the acquired T2w images and the corresponding T2 volume. Representative T2w images for subject 2 (acquisition time: 10 min, heart-rate = 38 bpm), and the corresponding T2 maps obtained by the proposed 3D MUST-T2. Eight reformatted short-axis slices that cover the heart from apex to base are shown. Uniform distribution of T2 values through the slices over the whole-left ventricle can be observed. The color scale indicates T2 values between 0-120 ms.

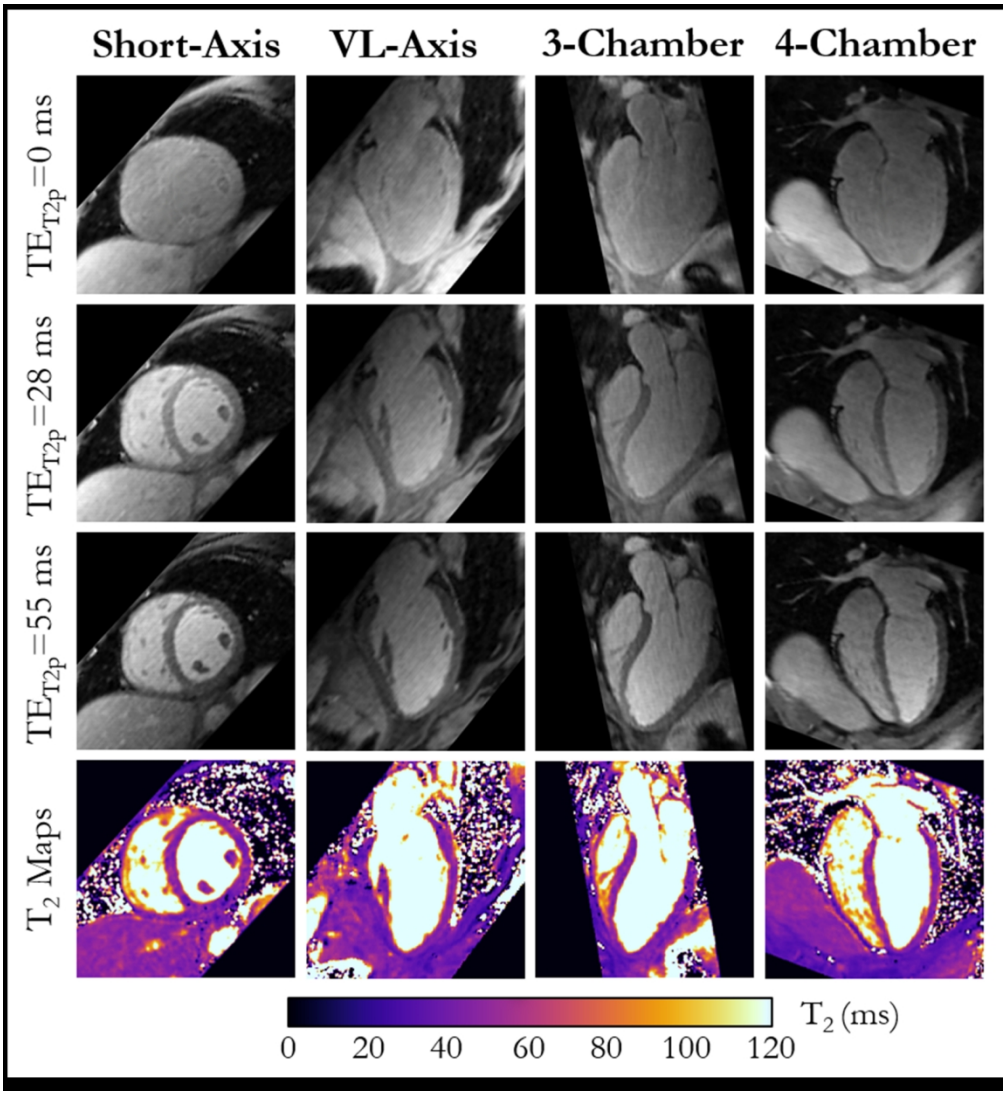

Figure 7. Representative T2-prepared images for subject 2 and the corresponding T2 maps obtained with the proposed 3D MUST-T2 sequence. Reformats in short-axis, vertical long-axis, 3-chamber and 4-chamber views are shown.

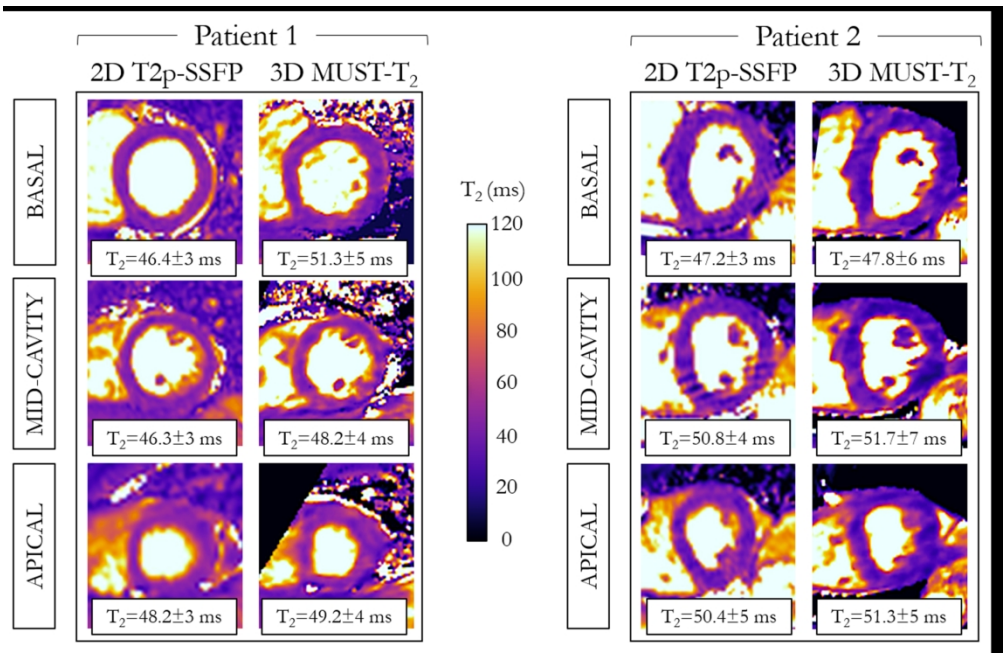

Figure 8. Short-axis T2 maps at apical, mid-ventricular and basal level for two patients acquired with the proposed free-breathing 3D MUST-T2 framework and the conventional breath-hold 2D T2p-SSFP sequence. The septal T2 relaxation times for each slice are reported as mean ± standard deviation.

228x147mm (300 x 300 DPI)